



# UNIVERSITAT DE BARCELONA

Final Degree Project  
**Biomedical Engineering Degree**

**“Development of an open-source,  
wireless and implantable vagus nerve  
stimulator for preclinical studies in mice  
(Stage II)”**

Barcelona, January 20, 2022  
Author: Carla García Hombravella  
Director/s: Dr. Antoni Ivorra  
Dra. Laura Becerra-Fajardo  
Tutor: Dr. Agustín Gutiérrez-Gálvez

## **Acknowledgements**

To my two directors Dr. Antoni Ivorra and Dra. Laura Becerra-Fajardo who, from the moment I contacted, deposited their trust in me. For their guidance, advice, and support; their time, their patience and kindness.

To the rest of the members of the Biomedical Electronics Research Group for their hospitality and help.

To Dr. Agustín Guitérrez-Gálvez who has accompanied me as a teacher in several subjects during the degree and now as my tutor at the end of this journey, thank you.

## **Abstract**

Vagus nerve electrical stimulation (VNS) consists in delivering electrical impulses to the vagus nerve. VNS is an established therapy for epilepsy and drug-resistance depression, and it has shown great potential for other neurological and non-neurological disorders. Long-term vagus nerve stimulation research in rodent models is key for progress in treatments that are based on it. However, access to implantable vagus nerve stimulators for experimentation is very limited. The development of an open-source, wireless and implantable vagus nerve stimulator for preclinical studies in mice has been proposed. The stimulator must fulfil highly demanding requisites regarding volume and weight which challenge the electronics, especially consumption-wise, leading to unreasonably short battery lifespans. This final degree project is the second stage of the stimulator's development and addresses this trade-off between the minimization of volume and weight and current consumption, providing it with its optimal 3D design and electronic activation protocols. The final proposal in this work has a volume of 389.35 mm<sup>3</sup>, weighs 1.251 g, and lasts up to 12.32 days of uninterrupted stimulation following the FDA protocol for epilepsy.

**Keywords:** Vagus nerve stimulator, implantable, minimization, consumption.

# Table of Contents

<b>List of figures</b> .....	<b>6</b>
<b>List of tables</b> .....	<b>8</b>
<b>1. Introduction</b> .....	<b>9</b>
1.1. Motivation of the global project.....	9
1.2. Objectives .....	9
1.3. Scope and Span.....	10
<b>2. Background</b> .....	<b>11</b>
2.1. The human nervous system and the vagus nerve.....	11
2.1.1. Vagus nerve physiology.....	11
2.1.1.1. Anatomy.....	11
2.1.1.2. Functions.....	12
2.1.1.3. Fibres .....	12
2.1.2. Stimulation of the vagus nerve.....	12
2.1.2.1. Vagal branches involved in VNS .....	13
2.1.2.2. Type of fibres involved in VNS .....	13
2.1.2.3. Parameters of stimulation.....	14
2.2. Description of the situation (Stage I of the project).....	16
2.3. State of the Art .....	18
<b>3. Market analysis</b> .....	<b>19</b>
3.1. Market drivers and restraints.....	19
3.2. Market segmentation.....	19
3.3. Key industry players .....	20
<b>4. Conception Engineering</b> .....	<b>21</b>
4.1. For the minimization of volume and weight .....	21
a) Revision and reselection of electronic components .....	21
b) 3D design of the stimulation board.....	21
c) Study of the behaviour of the evaluation circuit using the new components .....	21
4.2. For the minimization of consumption and optimization of the battery's lifespan .....	22
a) Study of current consumption and timings of different blocks of the circuit, their activation and deactivation.....	22
b) Protocol design for the activation of the different blocks aiming to optimize consumption.....	22
c) Battery's lifespan estimation.....	22
<b>5. Detail Engineering</b> .....	<b>23</b>
5.1. For the minimization of volume and weight .....	23
a) Revision and reselection of electronic components .....	23
b) 3D design of the stimulation board.....	24

c)	Study of the behaviour of the evaluation circuit using the new components .....	25
5.2.	For the minimization of consumption and optimization of the battery's lifespan .....	32
a)	Study of current consumption and timings of different blocks of the circuit, their activation and deactivation.....	32
b)	Protocol design for the activation of the different blocks aiming to optimize consumption.....	39
i.	FDA guideline for epilepsy .....	39
ii.	Rodent model treatment suggested in [21].....	42
c)	Battery's lifespan estimation.....	44
5.3.	Results .....	44
<b>6.</b>	<b>Execution Chronogram (GANTT).....</b>	<b>46</b>
6.1.	Execution Chronogram of the Global Project .....	46
6.2.	Execution Chronogram of Stage II of the global project.....	47
<b>7.</b>	<b>Technical feasibility: SWOT analysis.....</b>	<b>49</b>
	Internal Analysis.....	49
	External Analysis.....	49
<b>8.</b>	<b>Economical feasibility .....</b>	<b>51</b>
<b>9.</b>	<b>Regulations and legal aspects.....</b>	<b>52</b>
<b>10.</b>	<b>Conclusion and future lines.....</b>	<b>53</b>
<b>11.</b>	<b>References.....</b>	<b>54</b>
<b>12.</b>	<b>Annex.....</b>	<b>57</b>

## List of figures

<b>Figure 1.</b> Structure of the human nervous system.	11
<b>Figure 2.</b> Typical charge-balanced, current waveforms used in neural stimulation. Cathodic current ( $I_c$ ). Anodic current ( $I_a$ ). The stimulation of this VNS corresponds to the monophasic capacitor-coupled stimulation (subplot c). Extracted from [31].	15
<b>Figure 3.</b> Sketch of the building blocks of the implantable vagus nerve stimulator. Extracted from [34].	16
<b>Figure 4.</b> Schematic of the Stimulation Circuit.	17
<b>Figure 5.</b> Stimulation Block timeline: MOSFET controls.	17
<b>Figure 6.</b> Schematic of the Voltage Booster Block.	17
<b>Figure 7.</b> Harald Strauss implantable nerve stimulator for mice.	18
<b>Figure 8.</b> Invilog Research Ltd. implantable nerve stimulator for mice and rats.	18
<b>Figure 9.</b> Stimulation board. Distribution of its main components. Top view.	24
<b>Figure 10.</b> Stimulation board. Distribution of its main components. Bottom view.	24
<b>Figure 11.</b> 3D design of the stimulation board with its main components. Top left view, bottom right view and front view.	25
<b>Figure 12.</b> LTspice schematic for the simulation of the Voltage Booster Block.	26
<b>Figure 13.</b> Output of the simulation of the Step-Up Converter	26
<b>Figure 14.</b> LTspice schematic for the simulation of the stimulation pulse generation.	27
<b>Figure 15.</b> Output of the simulation of the Stimulation Block. Stimulation pulses of 1 mA in red. MOSFET1 and MOSFET2 control in green and blue, respectively. Charge and discharge of the blocking capacitor in turquoise.	27
<b>Figure 16.</b> Monophasic capacitor-coupled stimulation pulses of 1 mA of the VN stimulator	28
<b>Figure 17.</b> Electronic circuit to check functionality of MOSFET2.	29
<b>Figure 18.</b> Screen shot of the oscilloscope. Voltage across the output load (12 k $\Omega$ ) for stimulation pulses of 1 mA. In yellow, the voltage drop at the electrodes. In blue, MOSFET1 control. In green, MOSFET2 control.	29
<b>Figure 19.</b> Screen shot of the oscilloscope. Zoom into a single stimulation pulse of 1 mA. In yellow, the voltage drop at the electrodes. In blue, MOSFET1 control. In green, MOSFET2 control.	30
<b>Figure 20.</b> Voltage compliance. Changes in the output current of 1 mA as $R_L$ increases.	31
<b>Figure 21.</b> Simulation of the decay of the stimulation current due to the impeded discharge of the blocking capacitor. Charge of the blocking capacitor in turquoise. Stimulation current in red.	32
<b>Figure 22.</b> Voltage Booster Block. PCB schematic.	33
<b>Figure 23.</b> Plots of the $V_{out}$ response and current consumption at the first activation of the Step-Up Converter	34
<b>Figure 24.</b> Screen shot of the oscilloscope. Voltage drop of the current source in blue. $V_{out}$ of the Step-Up Converter in yellow.	35
<b>Figure 25.</b> Plot of the decay of the 20 V of the Step-Up Converter's output with time without SHDN deactivation	36

<b>Figure 26.</b> Plots of the Vout response and current consumption at the deactivation of the Step-Up Converter	37
<b>Figure 27.</b> Plot of the reactivation of the Step-Up Converter after having decayed to 12.2 V since its deactivation.	37
<b>Figure 28.</b> Plots of the Vout response and current consumption at the reactivation of the Step-Up Converter starting at 12.2 V.	38
<b>Figure 29.</b> Screen shot of the oscilloscope. Vout of the Step-Up Converter in purple (5 V/div). Voltage at SHDN pin in green (5 V/div). Stimulation pulses in blue (5 V/div). Phase A and start of phase B of the stimulation protocol for FDA guideline.	40
<b>Figure 30.</b> GANTT diagram of the global project of the development of an implantable vagus nerve stimulator. In darker orange Stage II constitutes this TFG.	46
<b>Figure 31.</b> GANTT diagram of Stage II of the global project.	48

## List of tables

<b>Table 1.</b> VNS guidelines considered in this VN stimulator.	15
<b>Table 2.</b> Components of the vagus nerve stimulator.	23
<b>Table 3.</b> Voltage compliance: changes in the output current of 1mA as RL increases.	31
<b>Table 4.</b> Consumption phases of the optimal protocol for delivering the treatment according to the FDA stimulation guideline. Where the first pulse is delivered at $t_0 = 0$ . Where $i \in [1,22]$ and is the number of repetition of the phase (counter).	41
<b>Table 5.</b> Consumption phases of the optimal protocol for delivering the treatment according to the FDA stimulation guideline. Where the first pulse is delivered at $t_0 = 0$ . Where $i \in [1,22]$ and is the number of repetition of the phase (counter).	43
<b>Table 6.</b> Summary of consumption phases of the Voltage Booster Block.	45
<b>Table 7.</b> Tasks involved in the realization of the <i>global</i> project of the development of an implantable vagus nerve stimulator.	46
<b>Table 8.</b> Tasks involved in this TFG the <i>Stage II</i> of the <i>global</i> project.	47
<b>Table 9.</b> SWOT analysis of the global project of the development of an implantable vagus nerve stimulator.	49
<b>Table 10.</b> Costs of the products and total cost of Part II of the project.	51



## 1. Introduction

### 1.1. Motivation of the global project

Vagus nerve electrical stimulation (VNS) consists in delivering electrical impulses to the vagus nerve. It is a widely implemented and FDA approved therapy for intractable cases of epilepsy and drug-resistance depression [1] [2]. Additionally, the range of disorders that are favoured by VNS is expected to expand, as it has shown promising results in the treatment of Alzheimer's, cardiovascular disorders, sepsis, and diabetes, among others [3]. Despite its promising future, some of the mechanisms of VNS remain yet unclear and further investigation needs to be carried out to identify its long-term benefits and side effects with precision. Rodent models with prolonged VNS instrumentation are therefore essential. By avoiding head-mounted devices or tethering, an implantable device allows chronic stimulation and does not interfere in the common behaviour of the mouse once it is implanted. However, the existing miniaturized implants lack the experimental requirements of long-term, in vivo stimulation.

This is the second final degree project (TFG) of a TFG series that gives a response to this problem aiming to develop a competent, open-source, wireless and implantable vagus nerve (VN) stimulator.

The first TFG of this project was conducted by Marcos Chic, a former Biomedical Engineering student of the Universitat Pompeu Fabra. During his work, which will be referred as Stage I of the project, Marcos made a first design of the electronic structure of the stimulator (see 2.2. *State of the situation* for details). However, the stimulator must fulfil highly demanding requisites regarding volume and weight, narrowing the selection of components to only a few that do not possess the best electronic characteristics, especially consumption-wise, leading to a very short battery lifespan. In Stage I the basic architecture of the implantable VN stimulator is defined. The next stages, including this Stage II, will study the architecture in detail to fine-tune its behaviour, creating a more reliable and efficient device.

### 1.2. Objectives

This TFG (Stage II) proposes to equilibrate the trade-off between the minimization of both consumption and volume of the stimulator. To achieve this goal, the specific objectives of this TFG are:

- Minimization of the volume and weight:
  - o Reselection of electronic components
  - o Spatial distribution of components: design of the stimulation board
- Minimization of current consumption and elongation of battery lifespan:
  - o Calculation of the consumption for the different activation phases of the stimulator
  - o Design of activation protocols to minimize the consumption
  - o Selection of the best protocol

### 1.3. Scope and Span

This is the Stage II TFG of a TFG series that altogether compose an integral project that develops a competent, open-source, wireless and implantable stimulator for preclinical studies in mice. The minimization of current consumption and the design of the optimal protocol to have the maximal lifespan of our stimulator, while competing for the most miniaturized and light structure, is the focus of this TFG. Its realization is key for the whole global project, which otherwise would be unprofitable. The scope of this project is in accordance with the accomplishment of its objectives, but also with the limiting fact that it is a final degree project and therefore has important time and economical constraints (see 6. *Execution Chronogram*).

The TFG includes:

- The 3D design of the VN stimulator.
- The acquisition of the chosen components (some with greater dimensions) and their soldering on to an evaluation board. The evaluation board is the non-miniaturized version of our stimulation board. As its name implies, its functionality is to evaluate all the components and circuit in bigger dimensions more economically before the development of the final miniaturized VN stimulator.
- The realization of simulations and experiments with the evaluation board for the fulfilment of the objectives. The electronic equipment available at the BERG (Biomedical Electronics Research Group) labs is used for this task (Arduino Uno, Oscilloscopes, Current Probes, etc).
- The programming for the calculation of consumptions and reproduction for different scenarios and protocols of stimulation.
- The choice making of the best protocol for stimulation.

The TFG excludes:

- The construction of the final miniature stimulation board.
- The programming of the chosen stimulation protocol in the MCU. The control of the stimulation protocol used for the TFG will be done in an Arduino Uno.
- The development of the cuff electrodes.
- The development of the stimulator's communication blocks for external wireless control.
- The design and fabrication of a newer version of the evaluation board with the enhancements that this TFG might propose as this will be covered by the next TFG.

## 2. Background

### 2.1. The human nervous system and the vagus nerve

The human nervous system is divided into the central nervous system (CNS), that comprises the brain and the spinal cord, and the peripheral nervous system, which comprises all nerves and ganglia outside the CNS. The peripheral nervous system is divided into the somatic nervous system and the autonomic nervous system. The somatic nervous system is under voluntary control, while the autonomic nervous system is a 'self-regulated' system which influences the behaviour of organs outside voluntary control, such as the heart rate, or other functions of the digestive system [4].

The autonomic nervous system has three branches: the sympathetic nervous system, the parasympathetic nervous system, and the enteric nervous system. The VN is the main component of the parasympathetic nervous system and innervates the heart, lungs, stomach, and liver, among others [5].

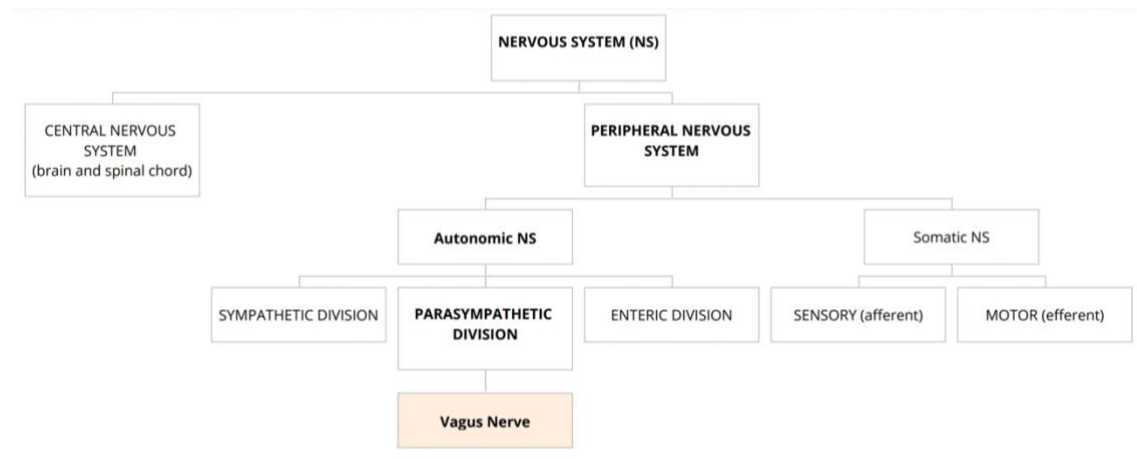


Figure 1. Structure of the human nervous system.

#### 2.1.1. Vagus nerve physiology

##### 2.1.1.1. Anatomy

The VN, also called pneumogastric nerve, is the longest and tenth cranial nerve (CN X), extending from the head to the abdomen [6]. Despite being referred as one single nerve, it in fact comprises two: the left and right vagus nerves.

It emerges from the medulla oblongata, the lower part of the brainstem. Within the cranium, an auricular branch arises, which supplies sensation to the posterior part of the external auditory canal and external ear. The VN exits the cranium via the jugular foramen and extends through the neck, at the end of which it divides into the right and left nerves. Many of its innervations are yet to be discovered, but the known ones can be divided into neck, thorax, and abdomen: (a) In the neck, several branches arise that provide innervation mainly to the pharynx, soft palate, and the larynx.

(b) As the nerve enters the thorax, it keeps on innervating the larynx, as well as the oesophagus, the lungs and the heart, regulating the heart rate and providing its visceral sensation (also known as interoception). (c) Finally, in the abdomen, branches supply innervation to the oesophagus, stomach, liver, pancreas and small and large bowel (duodenum and colon) [5] [7].

### **2.1.1.2. Functions**

The VN gives out motor parasympathetic fibres to all organs from the neck down to the second segment of the transverse colon, except for the adrenal glands. It also controls a few skeletal muscles, such as the muscles of the larynx, the pharyngeal muscles, and muscles from the palate and tongue [8]. It is therefore responsible for numerous and diverse tasks such as the lowering of heart rate, gastrointestinal peristalsis, sweating and muscle movements in the mouth, including speech. As beforementioned, it also has some afferent fibres that innervate the inner portion of the outer ear and part of the meninges.

Efferent VN fibres that innervate the pharynx and the back of the throat are responsible for the gag reflex. The VN is also involved in vomiting and in satiation after food intake [5] [9].

### **2.1.1.3. Fibres**

The VN is a mixed nerve, comprising both sensory and motor fibres. Approximately 80% of its fibres are afferent (sensory), carrying information from the body to the brain, and are originated at the nodose ganglion.

The rest are efferent (motor) pathways, which send signals from the brain to the body and are originated at the dorsal motor nucleus and nucleus ambiguus of the vagus [10] [11].

The VN is composed by A-, B- and C-type fibres, which differ in diameter and degree of myelination. Morphologically, A- and B-type fibres are myelinated, and have diameters of 5-20 and 1-3  $\mu\text{m}$  respectively, while C-type fibres are non-myelinated and have 0.4-2  $\mu\text{m}$  of diameter [12] [13].

## **2.1.2. Stimulation of the vagus nerve**

Vagus nerve stimulation (VNS) serves as treatment for different diseases, as it is believed to improve imbalance of autonomic control by increasing parasympathetic activity [14].

It is an approved therapy for intractable epilepsy and drug-resistant depression, and a potential one for many other diseases like heart failure, rheumatoid arthritis, inflammatory bowel disease, ischemic stroke, and traumatic brain injury [12].

Between the above mentioned, VNS is generally used to treat epilepsy for intervention-resistant patients. Meanwhile, for depression it remains a last resort option. In both cases, it is applied through a surgical implantation of a device with a battery and pulse-generator positioned below the collarbone connected to a wire that ends with an electrode wrapped around the left vagus nerve.

Despite having indisputably effective outcomes, there are potential perioperative risks involved with device implantation, such as bradarrhythmias during device placement, development of peritracheal hematoma (because of surgical trauma), and respiratory complications like vocal cord dysfunction and dyspnea (because of nerve trauma). Other VNS side effects are dysphonia, hoarseness, and cough, all of which may be mitigated by changing stimulus parameters [15].

### **2.1.2.1. Vagal branches involved in VNS**

Nowadays, clinical VNS is today only applied to the left cervical vagal trunk, which contains fibres from the recurrent laryngeal, cardiopulmonary, and subdiaphragmatic vagal branches.

Given the diversity of functions of VN branches, not all of them contribute to VNS seizure or disease suppression [16]. For example, an epilepsy study with mice showed that selective stimulation of the subdiaphragmatic branch alone is effective in epileptic seizure suppression [17]. However, it is not enough to discard a role for other branches in VNS.

There is also a debate about the stimulation in the right cervical branch. The left and right cervical branches differentially innervate the heart [18], having the right vagus nerve more direct projections to the cardiac atria [19] [20] and thus greater influence on heart rate. To avoid adverse cardiovascular effects in humans, the approved therapies limit to left-sided VNS [21]. However, there is no evidence that discards right-sided VNS from a safety nor an effectiveness point of view. Moreover, there is a hypothesis on the laterality of VNS effects in epilepsy: in a study published by Jansky et al. [22], 47 human patients with epilepsy were treated with left-sided VNS. A seizure-free outcome only resulted in patients who had lateralized interictal discharges; in other words, in patients that lacked bilateral interictal epileptiform discharges. This suggests that right-sided or bilateral VNS might be the alternative in patients that did not have an optimal outcome in left-sided VNS [16].

All things considered, there is an important gap of knowledge that leaves both safety and effectiveness of VNS in every vagal branch yet to be determined. These topics can be addressed in preclinical trials using the VN stimulator proposed in the TFG series that this TFG makes part of.

### **2.1.2.2. Type of fibres involved in VNS**

As explained above, the VN is composed by efferent and afferent nerve fibres, which are both involved in the clinically relevant effects of VNS [23]. At the same time, these are composed by the three types of fibres: A-, B- and C-type fibres. However, the effective stimulation in human VNS is thought to be primarily mediated by afferent vagal A- and B-type fibres, making C-type fibre stimulation non-necessary (at least in epilepsy) [24].

This is clinically relevant because the electrical thresholds for unmyelinated C-type fibres tend to be significantly greater compared to myelinated A and B-type fibres. The activation current threshold for C-type fibres is over 2 mA, while for A-type fibres it ranges from 0.02 to 0.2 mA and for B-type fibres from 0.04 to 0.6 mA [20].

Hence, the necessary amount of stimulation current is smaller, which also avoids unwanted side effects that could have made the therapy intolerable [14].

### 2.1.2.3. Parameters of stimulation

Current Strength: Stimulation of C-type fibres does not have clinical relevance and can increase the risk of suffering from side effects. The activation of these fibres that needs amplitudes of current above 2 mA tends to be avoided, and thus the current of stimulation is usually within the range between 0.5 and 2 mA.

Current Duration: The width of the pulses is related with the current amplitude, as the two parameters together determine the delivered charge. The relation between the two parameters is called strength-duration: the wider the pulse, the less amplitude that is needed to elicit an action potential. The minimum current amplitude for an infinite pulse duration that gives rise to the cellular depolarization threshold and an action potential is the rheobase current ( $I_r$ ). However, wide pulses increase the probability of tissue damage. Therefore, in the case of VNS, pulse widths do not overpass 1 ms [21].

Frequency: The indicated stimulation frequencies go from 20 Hz to 30 Hz [20] [25]. Prolonged stimulation frequencies over 50 Hz can provoke irreversible early axonal degeneration and therefore are avoided [26].

Duty Cycle: According to the FDA guidelines for treatment for people with epilepsy the duty cycle is of 30 s ON and 5 min OFF state. Other duty cycles for rodent models with different parameters suggest other ON and OFF times [21]. The two guidelines of stimulation that are thought to be the most important ones in investigation and that the present VN stimulator will be able to deliver are indicated in table 1.

GUIDELINE PARAMETER	FDA for epilepsy [20]	Rodent Model Treatment (Suggested in [21])
Amplitude ( $\mu$ A)	1000	500
Pulse width ( $\mu$ s)	500	250
Frequency (Hz)	20	10
Period (ms)	50	100

Duty Cycle (ON/OFF)	30 s ON / 5 min OFF	60 s ON / 5 min OFF
---------------------	---------------------	---------------------

**Table 1.** VNS guidelines considered in this VN stimulator.

Type of pulse: The pulses applied in VNS are usually symmetric square pulses: being the cathodic pulse followed by an anodic pulse in a charge-balanced manner [21] [27] [28] [29]. The cathodic pulse depolarises the tissue, provoking an action potential, while the anodic potential hyperpolarizes it. Biphasic pulses aim to avoid the arousal of Faradaic reactions that can trigger unwanted electrochemical processes [30]. However, in contrast with monophasic configurations (that deliver a depolarizing cathodic pulse alone), biphasic ones require more complex electronics, increasing volume (for instance, with two current sources instead of one). To avoid this complexity, the implemented configuration in this TFG is monophasic capacitor-coupled stimulation: the anodic wave is not rectangular like the cathodic one, but a peak representing the passive discharge of a dc-blocking capacitor (see figure 2). Despite allowing poorer control of the anodic wave, it avoids electronic components that limit the miniaturization.

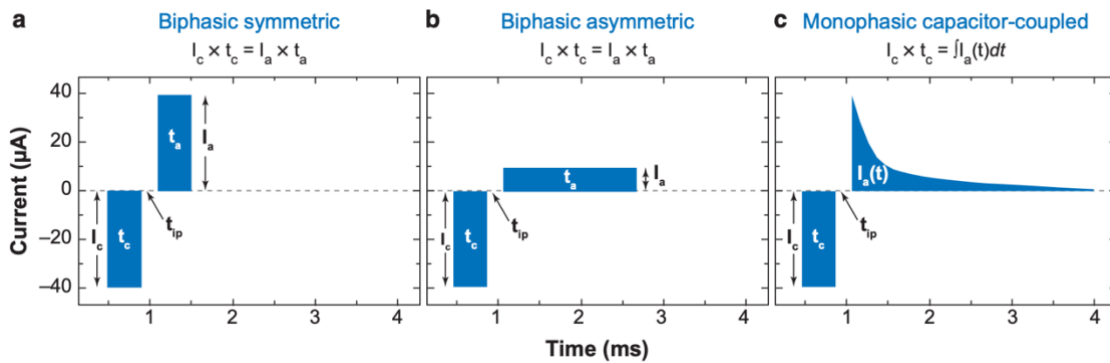


**Figure 2.** Typical charge-balanced, current waveforms used in neural stimulation. Cathodic current ( $I_c$ ). Anodic current ( $I_a$ ). The stimulation of this VNS corresponds to the monophasic capacitor-coupled stimulation (subplot c). Extracted from [31].

The pulse applied can be current-controlled or voltage-controlled. When voltage-controlled is applied, the voltage is fixed during the whole process, and the applied current depends on the impedance seen by the stimulator's electrodes (by Ohm's law). Voltage-controlled stimulation is therefore less precise, as there might be impedance changes at the electrodes for many circumstances (even if there is a partial detachment from the nerve) that will change the delivered current. For this reason, the stimulator of this TFG is a current-controlled stimulator, where the amplitude of the stimulation current is controlled (as mentioned, 1 mA or 500  $\mu$ A).

Type of electrodes: Finally, among the different electrodes available, this VN stimulator works with cuff electrodes that provide a fixed placement, avoiding detachments and drifts and improving the contact interface. Cuff electrodes also prevent current leaking out of the nerve, that could provoke unwanted charge injection to surrounding tissues [32] [33] [34].

## 2.2. Description of the situation (Stage I of the project)

The realization of the global project is motivated by the laboratory of Prof. Andrés Ozaita (Neuropharmacology Department Research Group), which studies the connectivity between brain regions during VNS and how they are affected. In this framework, the project is being developed through the mentioned TFG series at the Biomedical Electronics Research Group at the Pompeu Fabra University.

The work carried out during Stage I of the project consisted in the conception of the global project through extensive bibliographical research of VNS and an initial design and physical implementation of some of parts of the proposed VN stimulator. The conception of the stimulator's architecture is especially relevant for this TFG. The sketch of figure 3 shows the building blocks of the implantable stimulator proposed in Stage I of the project presented by Marcos Chic [34].

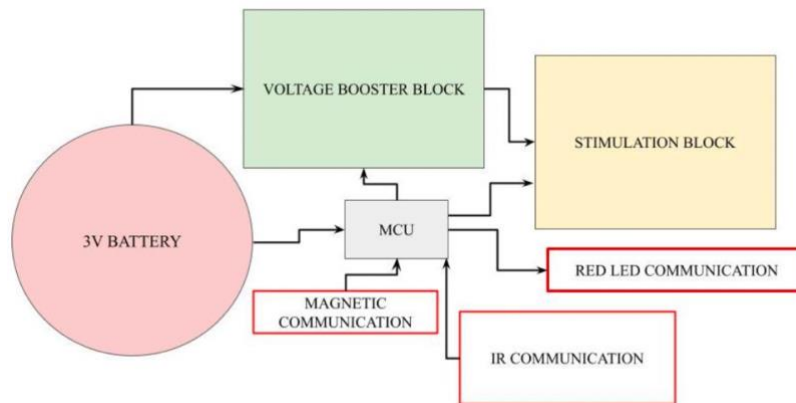


**Figure 3.** Sketch of the building blocks of the implantable vagus nerve stimulator. Extracted from [34].

Among the different blocks, the stimulation circuit (in yellow in figure 3) is the responsible of delivering the monophasic capacitor-coupled stimulation, and its schematic is detailed in figure 4. The fixed current is generated by a current source (Nexperia PSSI2021SAY) and can be regulated by an external programable resistance ( $R_{prog}$ ) or potentiometer. When a control voltage is supplied to the gate of MOSFET1, the current source is activated for a duration equal to the defined stimulation pulse width, the cathodic pulse is delivered to the electrodes at the vagus nerve, and a dc-blocking capacitor ( $C_{12}$ ) is charged. Then, MOSFET1 is turned off and MOSFET2 is activated, and the discharge of the blocking capacitor is activated through the electrodes and the tissues, generating the anodic wave (figure 5). The MOSFET transistors are to be controlled with a microcontroller unit.



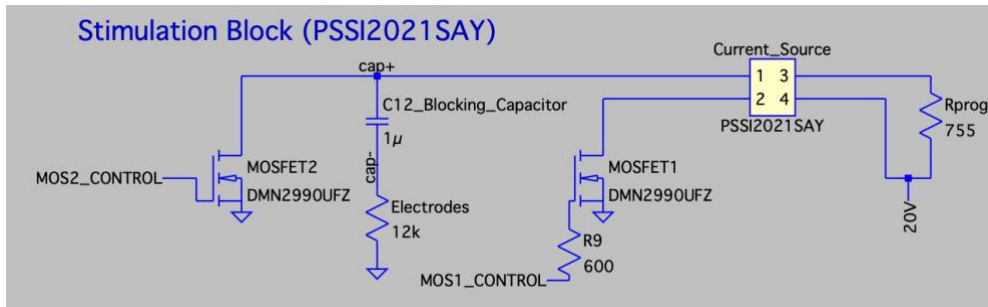


**Figure 4.** Schematic of the Stimulation Circuit.

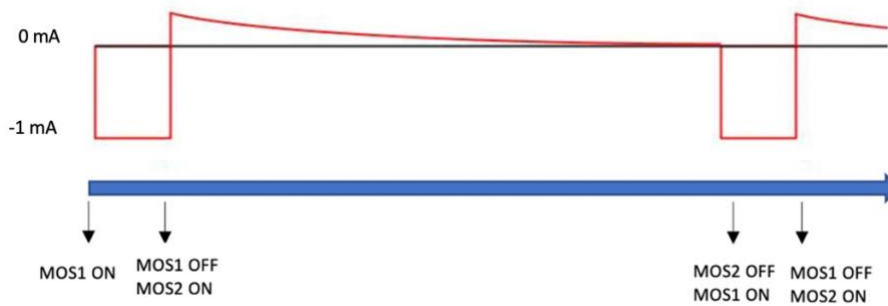


**Figure 5.** Stimulation Block timeline: MOSFET controls.

To guarantee this current amplitude, a minimum compliance voltage that depends on the resistance of the electrodes is needed. The impedance of cuff electrodes in cervical vagus nerve is between  $5\text{k}\Omega$  and  $15\text{k}\Omega$  [35] ( $12\text{k}\Omega$  are considered in this TFG). As it is observed in figure 4, 20 V of supply voltage were selected, this value will be discussed further sections. Given that our battery supply is of 3V, a Voltage Booster Block is necessary (figure 6), based on a Step-Up Converter (*Analog Devices LT3467*).

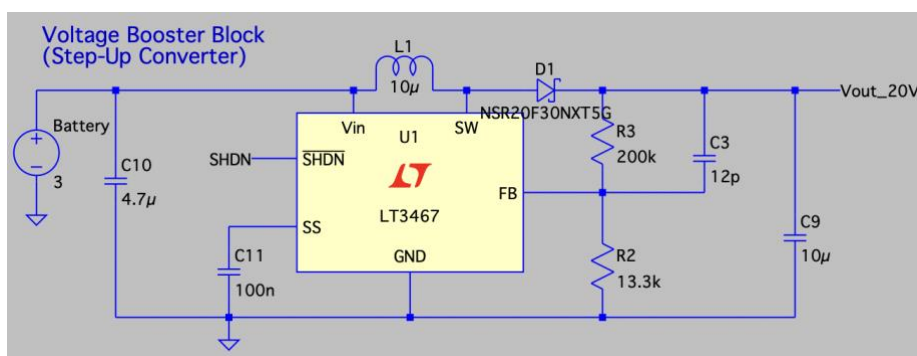


**Figure 6.** Schematic of the Voltage Booster Block.

Also, the magnetic, infrared, and red led communications that are included in figure 3 are to provide external wireless control of the stimulator. The development of these communication blocks were neither covered at Stage I nor in the present TFG.

In Stage I of the project, an evaluation board (i.e. “big vagus nerve stimulator”) was designed and developed. This is the electronic board used in this TFG (see 12. *Annex* for the schematics).

### 2.3. State of the Art

As stated, chronic VNS is a safe and a very effective treatment for patients with refractory epilepsy. VNS is also promising in a variety of other pathologies including major depression, Alzheimer disease, congestive heart failure (HF), bowel inflammatory disorders among others.

The state of the art is focused on increasing safety and effectiveness in the treatment for epilepsy and in VNS therapies used for these variety of pathologies which are not yet clinically implemented. Nowadays, there are two commercially available implantable VN stimulators for preclinical studies in mice [34]. The first one (figure 7) is offered by [Harald Straus Scientific](#) [36] but is currently distributed by the Burrell College of Osteopathic Medicine. It has a length of 15 mm, weights 1.2 g, and connects to a couple of coil electrodes. It applies voltage-controlled biphasic pulses of maximum 3 V with a maximum frequency of 5 kHz. The device has six different stimulation configurations that can be changed through a magnetic switch. Nowadays it has a prize of US\$ 250. The second one (figure 8) is commercialized by [Invilog Research Ltd.](#) It has a diameter of 13 mm, thickness of 3 mm and weights 1.4 g. The stimulation is current-controlled with monophasic pulses. It can reach a maximum of 18 V and 500 Hz and can be switched ON and OFF remotely. The stimulator costs 550 € but is sold in batches of six, having a total prize of 3300 €.

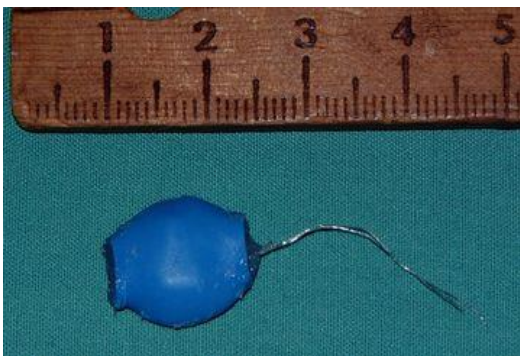


**Figure 7.** [Harald Straus Scientific](#) implantable nerve stimulator for mice.



**Figure 8.** [Invilog Research Ltd.](#) implantable nerve stimulator for mice and rats.

These two stimulators are based on classic stimulation models. However, current VNS investigation aims to breaks old paradigms betting on selective stimulation [37] [38], VN activity recordings [39], closed-loop control of the stimulation parameters [40] or new electrode design such as MEMS electrodes with polymer substratum [41]. These innovations are not yet confirmed by large clinical studies but might be the inception of next-generation VN stimulators.

### **3. Market analysis**

Epilepsy, treatment resistant depression and other neurological conditions are the primarily established applications of VNS and their patients are prime candidates for this therapy. An analysis of the global market of clinical VNS is carried out in this section. (The market analysis for the case of implantable systems for VNS experimentation in mice is contained in section 2.3.)

#### **3.1. Market drivers and restraints**

According to the World Health Organization (WHO), around 50 million people worldwide have epilepsy, and an estimated five million people are diagnosed with the condition each year [43]. China, India, and Brazil are among the countries with higher proportion of population suffering epilepsy. According to the WHO, 5% of adults suffer from different types of depression from which treatment resistance depression is growing prevalence [44]. This growing prevalence of neurological diseases, along with positive clinical results related to the use of VNS is what drives the market to grow.

Despite the increase in the incidence of epilepsy, depression, and other conditions, there are factors that restrain the growth of the market. One of them is lower treatment rates for neurological disorders in emerging countries, which limits the number of patients that undergo treatment which in addition usually have preference for regular medication. Another issue that limits the market is the high cost of the implantable VNS devices, along with the costs of the surgery [45] [46].

#### **3.2. Market segmentation**

The global VN stimulation market can be segmented according to the type of product, the application, and the geography.

By type of product, the VNS devices market is segmented into invasive and non-invasive (which are mainly transcutaneous VNS). The implantable and invasive VNS devices currently dominate over the non-invasive VNS.

In terms of application, the market is segmented into epilepsy and treatment resistant depression mainly. Other clinical applications of vagus nerve stimulation are migraine, apneas from obstructive sleep and headache. Several clinical trials are being carried out by research institutes to explore and expand applications of VNS. However, as mentioned, the established effectiveness of VNS in epilepsy and treatment resistance depression is the primary reason for dominance of these applications.

By geography, the leading VNS market is North America. This region has higher diagnosis and treatment rates for neurology, combined with adequate reimbursements policies for VNS devices. Additionally, there is patient's awareness of new treatments and availability of advanced VN stimulators in the region. The regions that are behind are Europe and Asia Pacific, whose market is expected to have significantly grown by 2026. The market in Latin America, Middle East and Africa is just at its beginning.

### **3.3. Key industry players**

The major player in the competition for the VNS market is LivaNova PLC. The company has a wide product portfolio of implantable VNS devices, from which the SenTiva™ is the best latest FDA approved VNS system. Other important key players are Medtronic PLC., Bio Control Medical, Electro Core LLC, Boston Scientific Corporation and Entero Medics LLC.

To conclude this section, the global market size for VNS was US\$ 505.2 million in 2018 and is projected to reach US\$ 1194.4 million by 2026, exhibiting a Compound Annual Growth Rate of 11.4 % during this period [45].

## 4. Conception Engineering

This section describes the approaches and methods that will be implemented in the TFG to achieve its objectives. The choice of these proposed solutions among the possible solutions is detailed below.

### 4.1. For the minimization of volume and weight

#### a) Revision and reselection of electronic components

The first step is to review the components chosen in Stage I of the project and examine their dimensions and their electronic characteristics. Then, extensive research of new components would be optimal to substitute the actual ones by others with the adequate electronic properties but with smaller dimensions. This can be done by examining what is offered by several distributors such as Mouser Electronics, Digi-key, and developers such as Texas Instruments, Analog devices, Renata... and examining the datasheet of the products to see whether their specifications fit in the requirements of our implantable VN stimulator.

#### b) 3D design of the stimulation board

Once the stimulator's definite components have been selected, the spatial distribution of the stimulation board must be designed. For it, a 3D modelling software platform must be used. The chosen software to carry out this task is the [Autodesk Fusion 360](#), on the grounds that it has been recommended by several professors and that it has a student license. At this point, several positionings of all the elements will be studied and the volume and weight must be calculated for each of them. The distribution that permits the best miniaturization will be selected.

#### c) Study of the behaviour of the evaluation circuit using the new components

The correct behaviour of the whole circuit with the new components must be ensured. In fact, if the results are not the expected ones, it will be necessary to go back to the first step and substitute the problematic components by other ones, also having to repeat the second step (design of the stimulation board). The focus will be set on the behaviour of the Step-Up Converter and of the Stimulation Block. In other words, it must be checked if the Step-Up Converter converts the 3V into 20 V correctly and if the Stimulation Block is able to deliver the stimulation pulses and under what conditions. This study will first be carried with simulation, using [LTspice XVII](#). The reason for which this software has been chosen among other SPICE software is because it includes models for many Analog Devices components (such as the Step-Up Converter) and because the author is already familiar with this software, and therefore no time must be devoted to learning its functioning. After the simulations are carried out, the behaviour will be checked experimentally. For the experimental set up, the smallest components will be soldered into a new evaluation Printed Circuit Board (PCB) using flux tack (Chipquick, SMD291) and an IR reflow oven, while the larger ones will be soldered using a soldering iron. The laboratory instruments that will be used for this task are the oscilloscope, a power source, a multimeter, among others. Moreover, MOSFET control to generate the pulses will be done through an [Arduino Uno](#) programmed using the [Arduino Software IDE](#).

Programming using [Visual Studio Code](#) editor will be done to make calculations and generate plots with the acquired data.

## **4.2. For the minimization of consumption and optimization of the battery's lifespan**

### **a) Study of current consumption and timings of different blocks of the circuit, their activation and deactivation**

To minimize the current consumption of the stimulator, firstly a study of consumptions and timings of the different blocks must be carried out. Just as in the previous steps, this will be first studied in simulations using LTspice and then the whole study will be carried out experimentally. For the current measurements two different methods will be tried out from which the best one will be chosen: measurement of electronic potential across a resistor and the calculation of the corresponding current using Ohm's Law, or the use of a current probe (TCP2020A from Tektronix, Inc). The key point will rely on examining the current consumption of the battery. Just like in previous steps, laboratory instruments will be used. To process, calculate and examine the electrical signals received at the oscilloscope, programming will be carried out. From the many programming languages and IDEs available, the author has chosen [MATLAB R2021a](#) because of personal preference.

### **b) Protocol design for the activation of the different blocks aiming to optimize consumption**

Once the consumption and behaviour of each block is known, different activation strategies will be studied taking into consideration the stimulation guidelines. The methodology will be based on examining the timings at which the blocks need to be active, and consider different activation strategies that ensure that the stimulation will be properly done and choose the strategy with the least current consumption. Experiments with such protocols will also be carried out to confirm the results of the calculations.

### **c) Battery's lifespan estimation**

From the best protocols, the lifespan of the battery will be calculated to know the days that the VN stimulator will be functioning after implantation.

## 5. Detail Engineering

### 5.1. For the minimization of volume and weight

#### a) Revision and reselection of electronic components

The first task carried out in this TFG was the improvement of the design of the implant proposed in Stage I of the project. As stated in 4. *Conception Engineering*, this was accomplished with the revision and update of the components of the implant and their optimal positioning, aiming to decrease as much as possible its total weight and volume. Extensive research of new components with smaller dimensions and that fulfilled the electronic requisites was done.

The final components of the implant can be observed in table 2. The main update regarding the components is the replacement of the previous inductor (4 x 4 x 3 mm) by a smaller one (3 x 3 x 1.5 mm). The new inductor was chosen under the indications specified in the LT3467 Step-Up Converter datasheet. The new inductor must handle currents of 1.2 A, must have low DCR (copper-wire resistance) to minimize power losses and must have an inductance between 4.7 and 10  $\mu$ H. The chosen inductor is the [Abracon ASPI-0315FS-4R7M-T2](#) and has an inductance of 4.7  $\mu$ H, in contrast with the 10  $\mu$ H of inductance the former had.

COMPONENT	DESCRIPTION	DIMENSIONS (mm)	WEIGHT (mg)
Renata CR1025	Battery	10 ( $\emptyset$ ) x 2.5	600
Abracon ASPI-0315FS-4R7M-T2	Inductor	3 x 3 x 1.5	94.039
Analog Devices AD5290	Digital Potentiometer	3 x 4.90 x 0.85	143.200
Analog Devices LT3467	Boost converter	3 x 2 x 0.75	212.421
Nexperia PSSI2021SAY	Current source	2.1 x 1.25 x 0.95	22
Kinetis KL03 MKL03Z8VFK4	Microcontroller	2 x 1.6 x 0.56	29.8
Würth Elektronik: 1541201EEA400	Photodiode	2 x 1.3 x 0.8	7.6
Analog Devices ADA4505-1	Operational Amplifier	0.9 x 1.38 x 0.6	-
Texas Instruments DRV5032	Hall Effect sensor	1.4 x 1,1 x 0.4	11
ON Semiconductor NSR10F40NXT5G	Schottky diode	1.4 x 0.6 x 0.3	0.521
Vishay 298D106X0025A2T	Tantalum capacitor	1 x 0.6 x 0.5	-
Diodes Incorporated DMN2990UFZ	MOSFET transistor	0.62 x 0.62 x 0.39	-
Kingbright APG0603SECETT	LED	0.65 x 0.35 x 0.2	-
Capacitors 0402 package	Capacitors (I)	1 x 0.6 x 0.2	-
Capacitors 0603 package	Capacitors (II)	1.6 x 0.8 x 0.8	-
Capacitors/resistances 0201 package	Capacitors/resistances	0.6 x 0.3 x 0.24	40

**Table 2.** Components of the vagus nerve stimulator.

**b) 3D design of the stimulation board**

Among the many distributions and sketches designed with the Autodesk Fusion 360 software, the definitive 3D design of the implantable vagus nerve stimulator with its main components is the one in figures 9, 10 and 11.

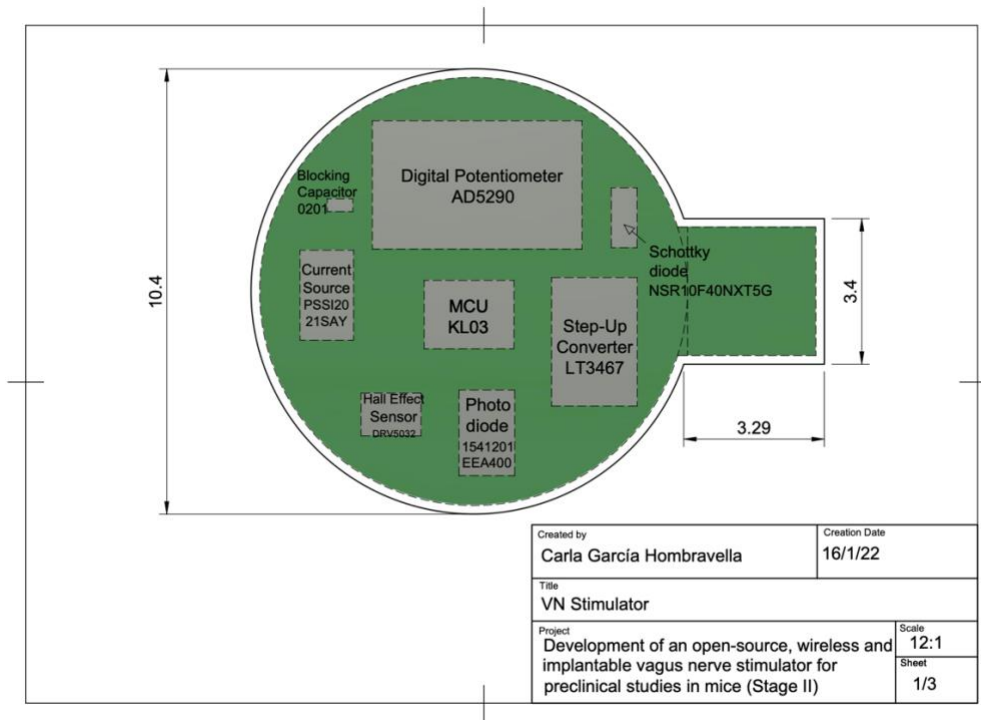


**Figure 9.** Stimulation board. Distribution of its main components. Top view.

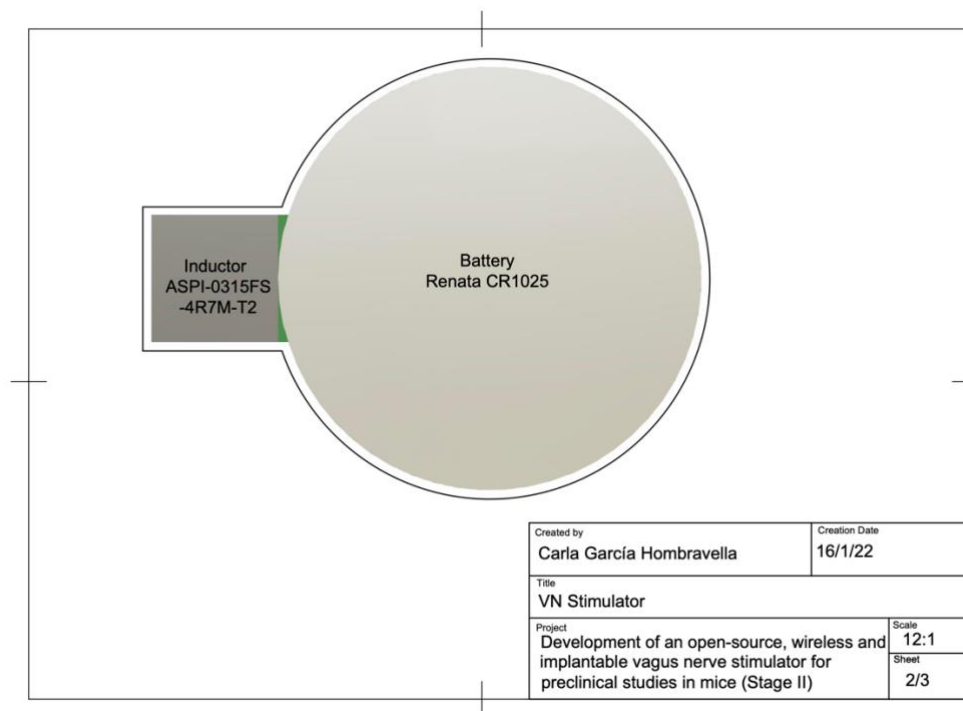


**Figure 10.** Stimulation board. Distribution of its main components. Bottom view.



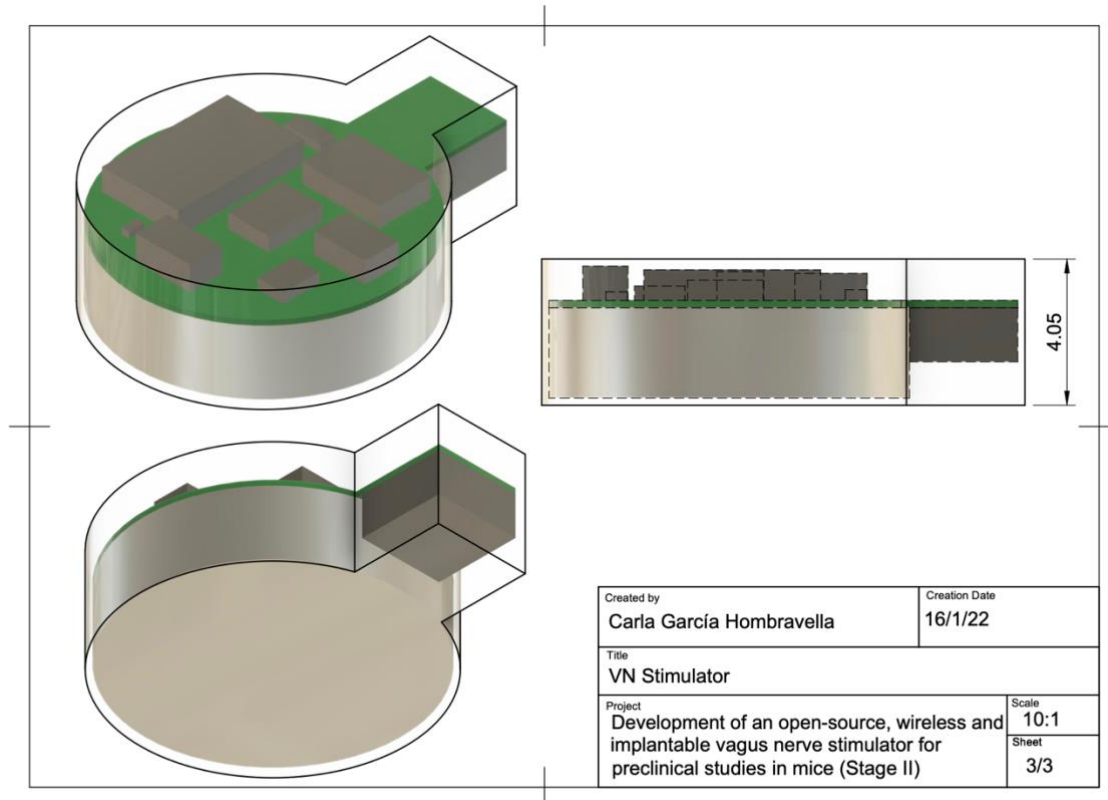


**Figure 11.** 3D design of the stimulation board with its main components. Top left view, bottom right view and front view.

The stimulator is built on a PCB of 0.2 mm of thickness. The battery will be placed at its bottom and most of the components at its top. The whole stimulator will be encapsulated in epoxy with minimum 0.2 mm of margin.

Despite having found a smaller inductor its height still takes over too much volume: it has 1.5 mm of height while the second highest element is the current source with 0.95 mm of height. To minimize this problem, the design (figures 9, 10 and 11) includes an appendix that permits the upside-down positioning of the inductor, reducing the total height of the stimulator and its total volume, specifically of epoxy, which reduces the weight as well. The upper part of the appendix will be occupied by capacitors and other very small components which do not appear in the 3D sketch. The appendix is where the wires for the electrodes will leave the implant.

The diameter of the stimulator (without counting in the appendix) is of 10.4 mm and it has a height of 4.05 mm. The final stimulator has a volume of 389.35 mm<sup>3</sup> and a weight of approximately 1.251 g. This weight may vary according to the choice of epoxy type, which will determine its density and therefore the contribution to the final weight. The considered epoxy is a light one with 0.8 g/cm<sup>3</sup> density. The density considered for the PCB is of 1.85 g/cm<sup>3</sup>.

**c) Study of the behaviour of the evaluation circuit using the new components**

To ensure that the new components permitted the correct behaviour of the stimulation, the corresponding simulations with LTspice and experiments were carried out.

i. Simulations

Before working with the actual evaluation board, LTspice simulations were made to assess the behaviour of the circuit with its new components.

The first subcircuit to simulate was the Voltage Booster Block, which outputs 20 V with an input of 3 V. As it can be observed in figure 12, the central component of the Voltage Booster Block is the LT3467.

The battery of the stimulator (Renata CR1025) has no LTspice model and a diode was placed after the voltage source as a current limiter of 30 mA, as this is the current limit indicated in the datasheet of the battery. Moreover, 48 kΩ are placed at the output, which is the internal resistor value of the current source that is connected to the output of the Voltage Booster Block. The output signal of the Step-Up Converter is observed in figure 13. The Step-Up Converter is able to reach 20 V after 40 ms with the new inductor and with the current limitation of the battery (which had not been tested before).

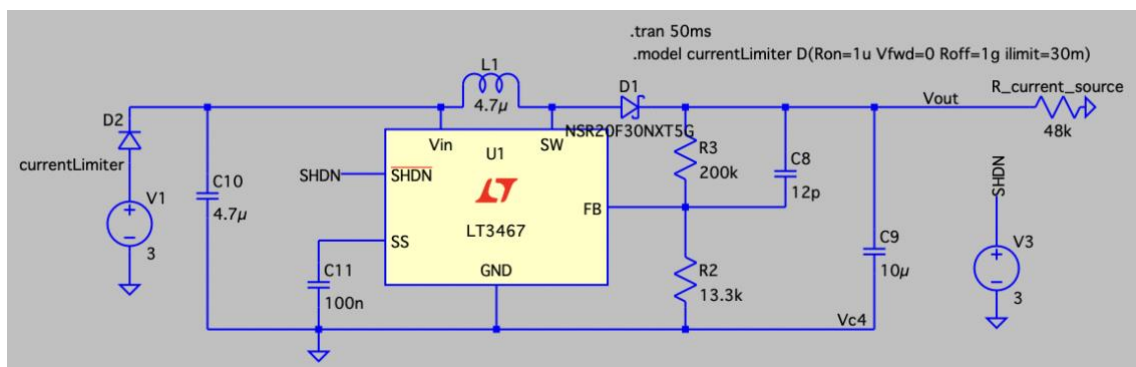


**Figure 12.** LTspice schematic for the simulation of the Voltage Booster Block.

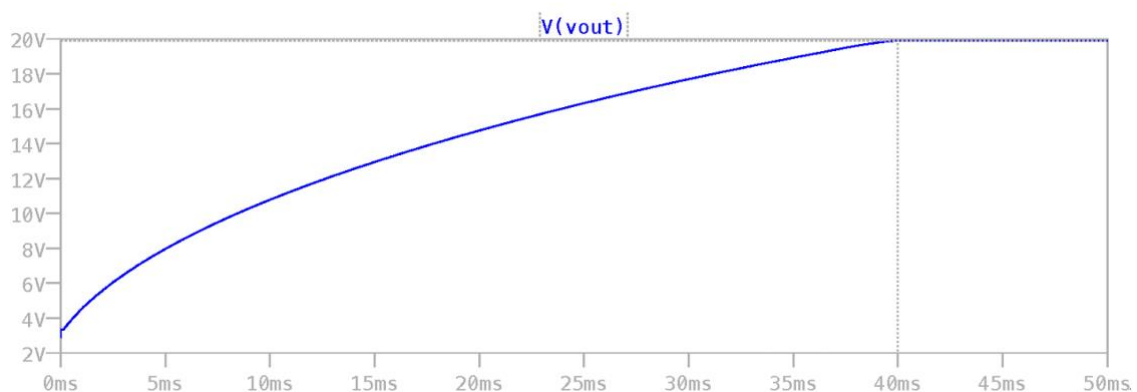


**Figure 13.** Output of the simulation of the Step-Up Converter

A second LTspice simulation was carried out to evaluate the current that will flow through the electrodes and the tissue (figures 14 and 15). As stated in 2.1.2.3. *Parameters of Stimulation*, the

FDA guideline for VNS in epilepsy are pulses of 500  $\mu$ s of 20 Hz. This stimulation pattern is controlled by the voltage pulses at the gate of the MOSFET transistors (see 2.2. *Description of the Situation (Stage I of the project)*). Rprog is set to 755  $\Omega$ , since it was decided to stimulate with 1 mA and a formula provided in the current source's datasheet permitted to compute this resistance value. Figure 16 shows that the shape of the stimulation pulses is indeed the one of monophasic capacitor-coupled stimulation pulses.

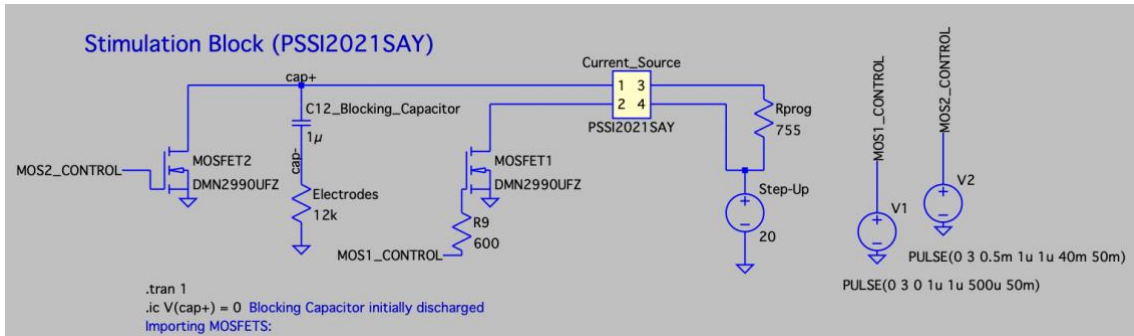


Figure 14. LTspice schematic for the simulation of the stimulation pulse generation.

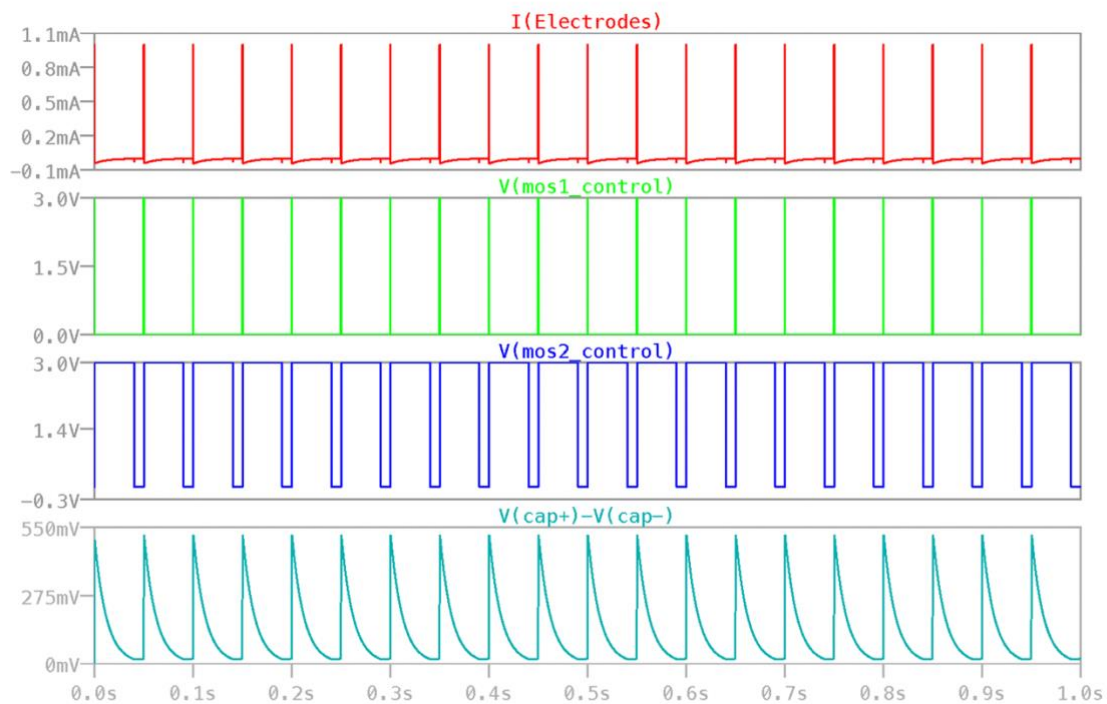
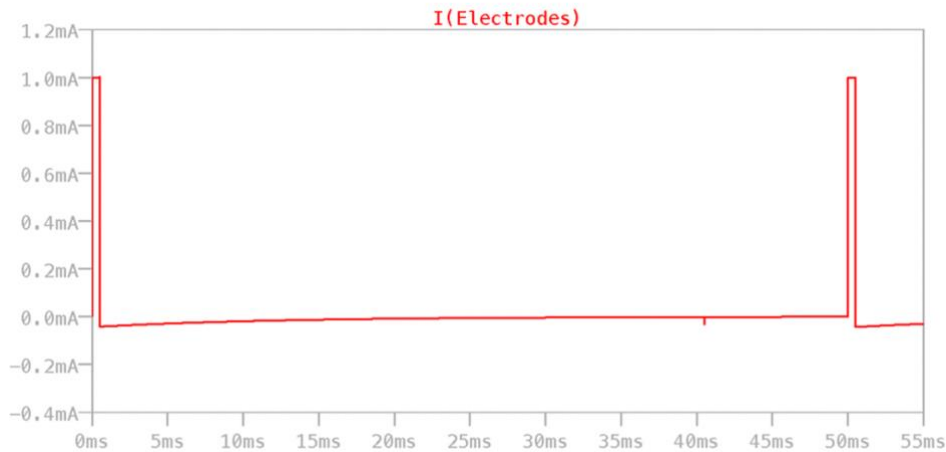


Figure 15. Output of the simulation of the Stimulation Block. Stimulation pulses of 1 mA in red. MOSFET1 and MOSFET2 control in green and blue, respectively. Charge and discharge of the dc-blocking capacitor in turquoise.



**Figure 16.** Monophasic capacitor-coupled stimulation pulses of 1 mA of the VN stimulator

Due to computational limitations, the two schematics could not be evaluated in a single schematic that included all the components' models as the simulation failed. The behaviour of the complete circuitry is tested in the experiments.

ii. Experiments

The new components were soldered into a PCB (see 12. Annex for images).

The output of the two blocks was examined experimentally. The reader may consult the schematics and layouts of the PCB in 12. Annex section. At this stage, the experiments were done with a power supply.

The Voltage Booster Block correctly outputted the 20 V after 5.22 ms of activation. This rapid raise is because the power supply has a greater current limit, set at 100 mA. However, as it will be shown in further sections, this rise is much slower when the voltage supply is delivered by the battery of the stimulator.

The behaviour of the Stimulation Block was also experimentally checked. However, in contrast with the Voltage Booster Block, the stimulation pulses did not appear correctly. The first stimulation pulse did indeed reach 1 mA, but this current decreased fast in the following pulses. This happened because the blocking capacitor was not discharging correctly when MOSFET2 was being activated. Many experiments were carried out to find the origin of the problem: The first experiment that was carried out was the generation of a single stimulation pulse (a single MOSFET1 activation) that charged the blocking capacitor. Then, the blocking capacitor was short-circuited to see if it had a correct discharge, which it did. Therefore, the problem relied on the behaviour of MOSFET2. To finally confirm that MOSFET2 was damaged (or not soldered correctly) the circuit of figure 17 was arranged.

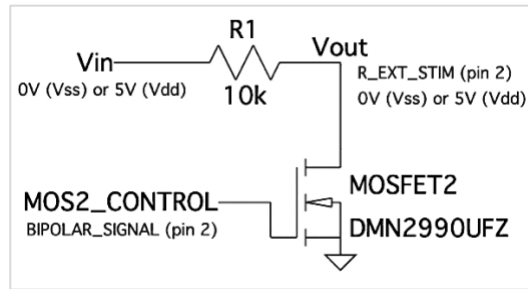


**Figure 17.** Electronic circuit to check functionality of MOSFET2.

When MOSFET2's gate was connected to ground, Vout equaled Vdd. However, when MOSFET2's gate was connected to Vdd, Vout did not fall to Vss. Therefore, MOSFET2 was damaged.

A new MOSFET2 was soldered to the circuit but again without success. In order to move forward with the project and achieve the TFG's objectives, an external NMOS (BS170 / MMBF170) was connected to the test points of the PCB. With this NMOS, the pulses were generated correctly (figures 18 and 19).

The signal recorded by the oscilloscope is the voltage drop between the two electrodes. Given that a resistance of 12 k $\Omega$  (simulating the tissue resistance) was connected across the electrode test points, and pulses of 12 V are obtained, the current of the pulses is the expected 1 mA. Again, the control of the pulses at the MOSFET gates is carried out with the Arduino Uno (see 12. Annex for codes).

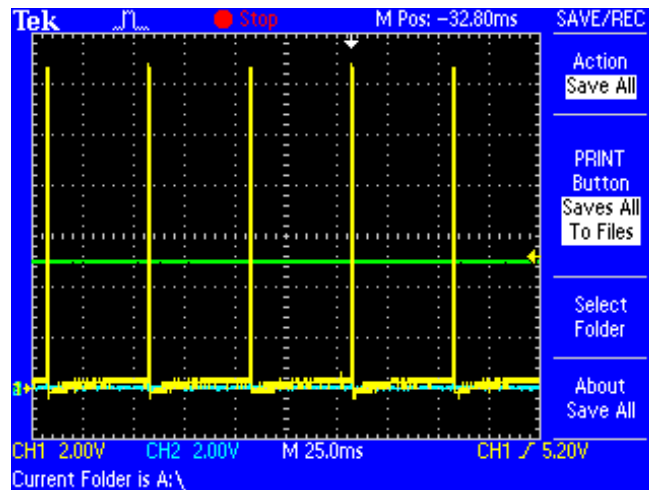


**Figure 18.** Screen shot of the oscilloscope. Voltage across the output load (12 k $\Omega$ ) for stimulation pulses of 1 mA. In yellow, the voltage drop at the electrodes. In blue, MOSFET1 control. In green, MOSFET2 control.

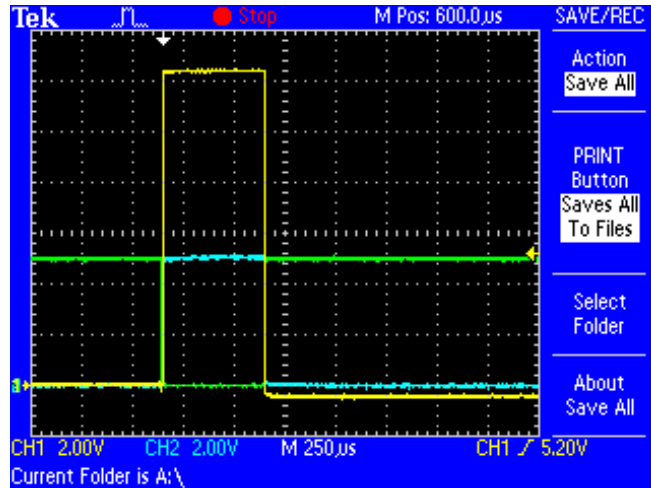


**Figure 19.** Screen shot of the oscilloscope. Zoom into a single stimulation pulse of 1 mA. In yellow, the voltage drop at the electrodes. In blue, MOSFET1 control. In green, MOSFET2 control.

### Phenomena that can jeopardize the stimulation pulse

There are two phenomena that can prevent the correct stimulation pulse generation and therefore must be taken into consideration.

#### (1) Voltage compliance

Firstly, the minimum voltage at the electrodes that permits the correct delivery of stimulation current was studied: if the impedance across the electrodes (load resistance ( $R_L$ )) is too high, the current of the stimulation pulse decays. This phenomenon was observed both in simulations and experimentally and is shown in table 3 and in figure 20.

IN SIMULATION		EXPERIMENTALLY		
RL (kΩ)	Stimulation Current I <sub>lds</sub> (mA)	Measured true RL (kΩ)	Voltage drop at RL V <sub>RL</sub> (V)	Stimulation Current I <sub>lds</sub> (mA)
5.2	1.001	5.18	5.2	1.004
10	0.999	9.78	9.75	0.997
12	0.998	11.95	12.01	1.006
15	0.997	14.71	14.85	1.045
18	0.996	17.7	17.87	1.01
20	0.960	19.9	19.24	0.967
22	0.875	21.6	19.3	0.894
24	0.803	23.9	19.3	0.808
26	0.742	25.9	19.3	0.745
28	0.689	27.7	19.3	0.697
30	0.644	29.9	19.3	0.645

**Table 3.** Voltage compliance: changes in the output current of 1 mA as RL increases.

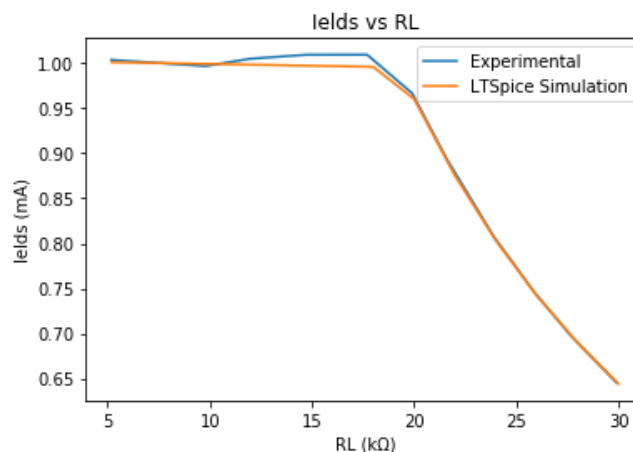


**Figure 20.** Voltage compliance. Changes in the output current of 1 mA as RL increases.

As the load resistance increases, so does the voltage drop between its ends ( $V_{RL}$ ). The voltage compliance is determined by the fact that the voltage drop at RL cannot be greater than the voltage provided at the output of the current source (i.e. the voltage at the output of the Step-Up Converter minus the voltage drop of the current source, set to approximately 20 V). When  $V_{RL}$  reaches values close to the voltage at the output of the current source (around 20 V), saturation occurs. The maximum value that RL can have without saturation ( $RL_{max}$ ) depends on the stimulation current  $I_{lds}$ , by Ohm's Law:  $V_{RL} = I_{lds} \cdot RL$ . Therefore larger  $I_{lds}$  have less tolerance for high electrode or tissue impedances RL.

This is important to set the voltage that is being outputted at the Step-Up Converter because, depending on the value of the delivered stimulation current  $I_{lds}$ , if we have too large tissue impedance, the stimulation current will decay if the provided voltage is not enough. Given that the considered load resistance is 12 kΩ, and the stimulation current is 1 mA, there is a margin that

even permits having less voltage than 20 V: 12 V at RL are sufficient (see next section 5.2.a) *Study of current consumption and timings of different blocks of the circuit, their activation and deactivation*).

## (2) Discharge of blocking capacitor

The second topic studied is the behaviour of the stimulation pulses when the blocking capacitor has not enough time to discharge. Again, the capacitor discharges during the MOSFET2 activation. Since the reduction of consumption is a major matter of this TFG, the reduction of the duration of the MOSFET2 pulses was initially thought as an approach to minimize it (in further sections it is indicated that this reduction of consumption is practically null).

What was seen is that the blocking capacitor is able to discharge as long as the control pulses of MOSFET2 have widths equal or wider than 5ms. In figure 21, simulations of the discharge of the blocking capacitor and the stimulation pulses are seen when the pulse at the MOSFET2 gate has a width of only 0.5ms. There is not enough time for the capacitor to discharge and it accumulates charge up to a certain level. The consequence of the incomplete capacitor discharge is the undesired decay of the stimulation current (which in this simulation was set to 1.2mA).

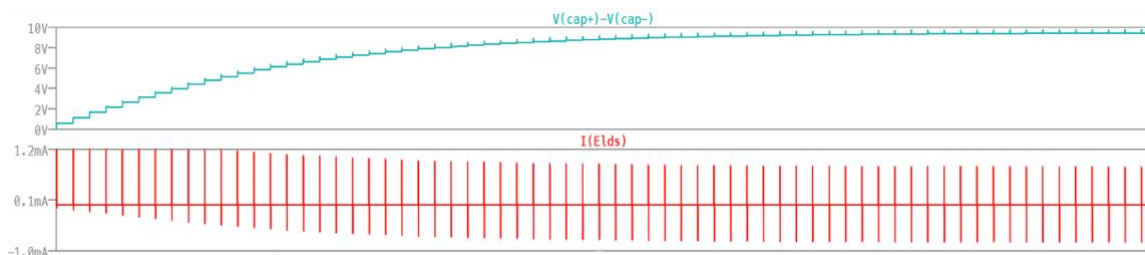


**Figure 21.** Simulation of the decay of the stimulation current due to the impeded discharge of the blocking capacitor. Charge of the blocking capacitor in turquoise. Stimulation current in red.

## 5.2. For the minimization of consumption and optimization of the battery's lifespan

### a) Study of current consumption and timings of different blocks of the circuit, their activation and deactivation

It is important to note that since the MCU and the potentiometer are not soldered in the PCB, their consumption is excluded in this study. The consumption current is studied mainly for the Voltage Booster Block (Step-Up Converter) and for the Stimulation Block.

Also, for this section, the results of the simulations were discarded for two reasons: 1) the computational saturation of the LTspice software when running many of the simulations, and 2) some of the components do not have a spice model and many approximations must be made that do not represent the circuit with reliability. For instance, in the simulation of figure 13 it was seen that the Step-Up Converter needed 40 ms to rise to 20 V, while in the experiments this rising time is larger (figure 23). Therefore, for the sake of reliability only the experimental results are taken as valid in this section.



The main subcircuit that needs to be activated is the Step-Up Converter (Voltage Booster Block), which outputs 20 V with an input of 3 V. The Step-Up Converter subcircuit is the one that appears in the schematic of figure 22.

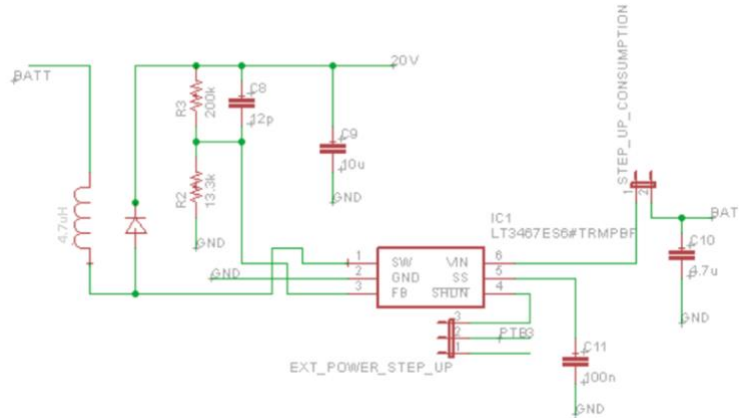


**Figure 22.** Voltage Booster Block. PCB schematic.

The component at the centre of the schematic is the LT3467.

The activation of this Step-Up Converter is controlled by the Shutdown pin (SHDN) of LT3467 (pin 4). The pin enables the device when tied to 2.4 V or more and shuts it down when it is tied to ground. Therefore, its evolution and consumption can be studied by activating and deactivating this SHDN with the battery voltage.

The presence of the 100 nF capacitor (C11) would enable the soft-start feature of the LT3467. The goal of this feature is to attenuate the inrush current drawn from the supply upon start-up, which otherwise could be too demanding for the battery. The designed circuitry in Stage I of the project contemplated this soft start capacitor. However, experiments without soft-start were carried out and concluded in the absence of an accentuated current peak at the activation of SHDN, which the battery could perfectly endure. Moreover, the attenuation of the inrush current with the soft-start feature is at the expense of a slower voltage rise and a significantly higher overall current consumption. Hence, this capacitor was removed, and all the presented results were carried out without it.

For the C9 capacitor, an electrolytic capacitor (Vishay 517D105M050JA6AE3) was set parallel to the originally used ceramic dielectric X5R capacitor, given that its performance falls off with such high tensions, and this of course affects rising and decay timings of the Step-Up Converter's output. In further stages of the project, the use of a tantalum capacitor instead must be considered, given that the electrolytic capacitor has too big dimensions and it is not appropriate for an implantable circuit.

Figure 23 shows the experiment in which SHDN is initially connected to ground and is then connected to 5V of the Arduino (note that the voltage at the SHDN pin is expected to be the 3V coming from the battery when the MCU is soldered and programmed). The consumption was measured with a current probe.

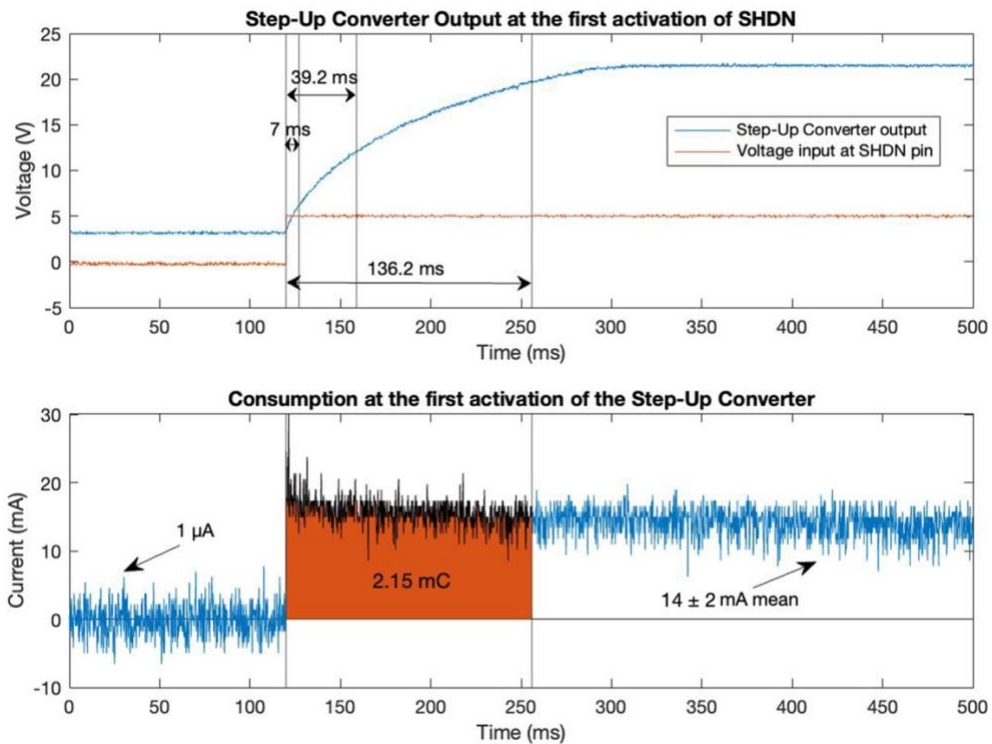


**Figure 23.** Plots of the  $V_{out}$  response and current consumption at the first activation of the Step-Up Converter.

It is observed in figure 23 that with the 3 V battery connected and SHDN deactivated, the output of the Step-Up Converter ( $V_{out}$ ) is of 3 V, as it is shut down and is only transferring its 3 V input to its output. Despite having the LT3467 deactivated, there is a basal battery consumption between 0.01 and 1  $\mu$ A. Such small order of consumption magnitudes can neither be observed experimentally or with simulation, and this value was taken from the datasheet of LT3467. The worst consumption scenario of 1  $\mu$ A is considered for the reliability of the results.

When the SHDN pin is activated,  $V_{out}$  immediately responds and starts rising. It takes 136.2 ms for  $V_{out}$  to reach 20 V (150 ms will be considered to leave margin for error). This is when the consumption current rises the most. As it is shown, it in fact keeps growing and reaches 21.2 V, leaving some margin. This can be adjusted with the values of the feedback resistors (see LT3467 datasheet). Since the activation of SHDN until  $V_{out}$  reaches 20 V, 2.15 mC of consumption were recorded with a maximum of 30.2 mA. Once it stabilizes over 20 V there is a mean of  $14 \pm 2$  mA of consumption. With time this consumption value and the battery voltage decrease slowly, but the Step-Up Converter will not be switched on enough time to notice it. Therefore, 14 mA of consumption is always expected at this stage of stabilization of the 20 V. The respective timings to reach 6.2 V and 12.2 V are 7 and 39.2 ms. The interest for these voltages is explained below.

Depending on which stimulation guideline is being implemented, the current that will flow through the electrodes will be set to 1 mA or 500  $\mu$ A. As explained with the voltage compliance, to have 1 mA current, since our RL is of 12 k $\Omega$ , a minimum of 12 V must be held at the output of the current

source. To deliver 500  $\mu\text{A}$  pulses, at least 6 V must be held at the output of the current source. However, the current source has a slight voltage drop, which means that to have 12 or 6 V at its output, its input voltage must be higher. The voltage drop at the current source was monitored experimentally and is of 200 mV (figure 24). This means that, despite having a Step-Up Converter configuration that reaches 20 V, as long as it outputs 12.2 V or more, 1 mA pulses of stimulation will be correctly provided. As long as the Step-Up Converter outputs 6.2 V or more, 500  $\mu\text{A}$  pulses of stimulation will also be provided successfully.

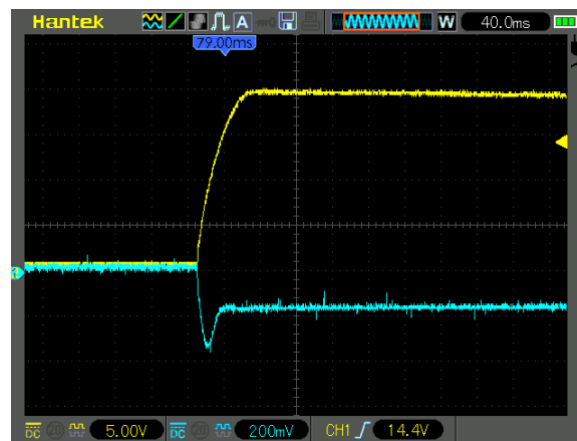


**Figure 24.** Screen shot of the oscilloscope. Voltage drop of the current source in blue. Vout of the Step-Up Converter in yellow.

The maximum time that the stimulator's battery permitted the maintenance of these 20 V was also examined with the oscilloscope. The experimental results are shown in figure 25.

The battery voltage drops from 3 V to 2.6 V when the output starts rising because of the consumption demand (this also happened with the soft-start capacitor). Since the SHDN input voltage is to be ruled by the MCU and supplied by the battery, this same voltage drop at the SHDN pin happens. This was not seen in the previous plots because SHDN was controlled and voltage supplied by the Arduino Uno, instead of having manually changed its pin from ground to the battery's voltage with a protoboard. The Arduino control was done to have a perfectly rectangular pulse, which otherwise was irregular, and could bias the calculation of the Vout rising time, among others. This irregularity is irrelevant for larger time periods like the one studied in figure 25, and the control was done manually. This voltage drop however does not prevent the output from reaching and holding the desired 20 V. This is also not a problem for the MCU that will be included in the implantable VN stimulator, as it operates above 1.71 V (see Kinetis KL03 MKL03Z32CAF4R by 299 NXP Semiconductors datasheet).

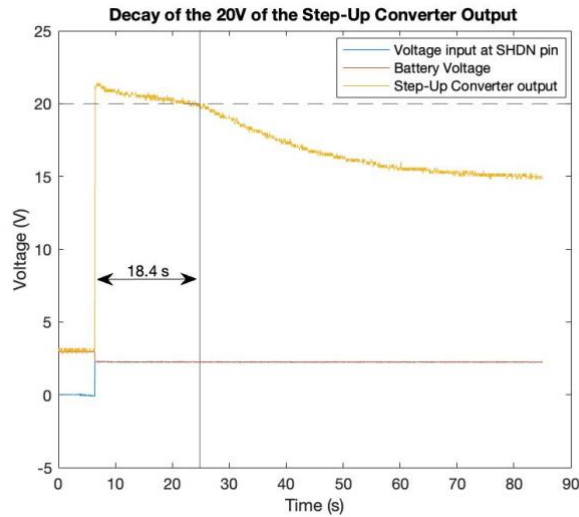


**Figure 25.** Plot of the decay of the 20 V of the Step-Up Converter's output with time without SHDN deactivation.

The 20 V can be maintained for 18.4 s. After this time, the output of the Step-Up Converter starts to decay.  $V_{out}$  is above 12.2 V and 6.2 V more time that can even be seen in the plot. Along with the rising time measures, this maintenance time will have to be considered when designing the protocols of activation of each phase. However, it is much more time than what the protocols rule (30 and 60 s ON) and therefore it does not put at risk the delivery of stimulation.

The response and consumption when SHDN is deactivated were also studied. The interest relies on the time that the voltage above 12.2 and 6.2 V is sustained after switching off. In other words, for how long the minimum 12.2 and 6.2 V are held after deactivating SHDN. This is useful because it permits an earlier switch off of the Step-Up Converter without having a negative impact on the stimulation, while saving up consumption. In figure 26 it is observed that this time is of 1.2 s for 12.2 V and 2.8 s for 6.2 V. Regarding the consumption decay, the consumption falls immediately with SHDN. Therefore, from the moment SHDN is deactivated, there is an instant drop to the 1  $\mu$ A basal consumption.

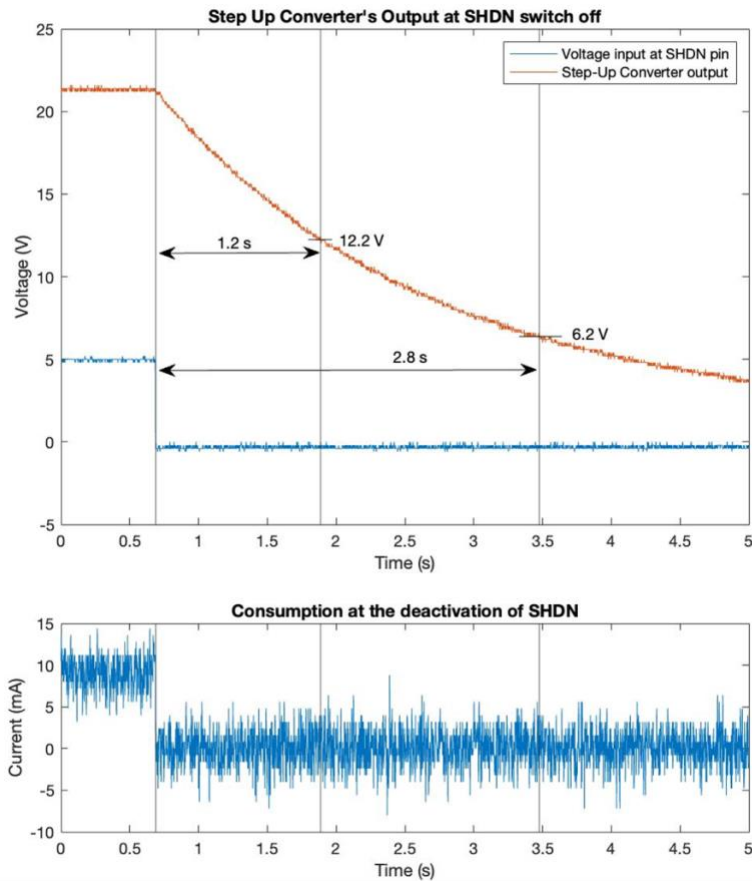


**Figure 26.** Plots of the  $V_{out}$  response and current consumption at the deactivation of the Step-Up Converter.

Because the consumption of having SHDN constantly on is very high ( $14 \pm 2$  mA), an option that will be considered in the activation protocols is switching SHDN off and switching it on again when it has decayed to 12.2 V and 6.2 V (minimum  $V_{out}$  for stimulation). This concept is shown in figure 27 with the rising from 12.2 V.

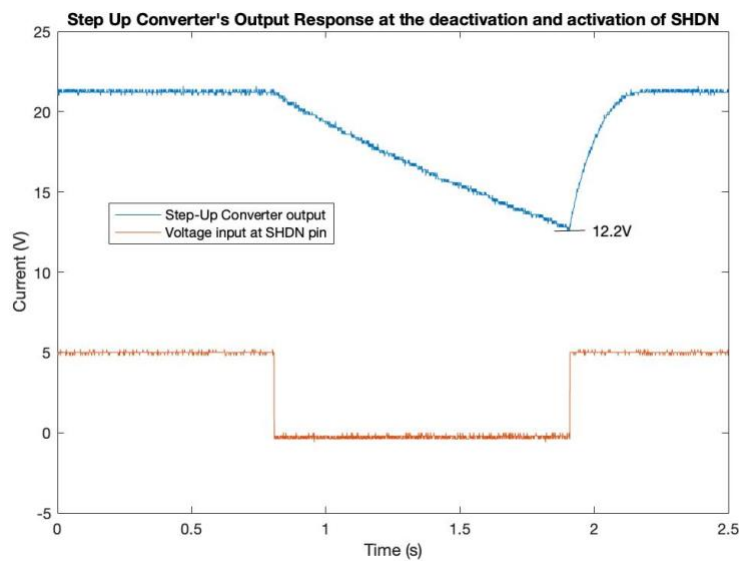


**Figure 27.** Plot of the reactivation of the Step-Up Converter after having decayed to 12.2 V since its deactivation.

The consumption and rising time when SHDN is activated from 12.2 V was also calculated and is shown with detail in figure 28.

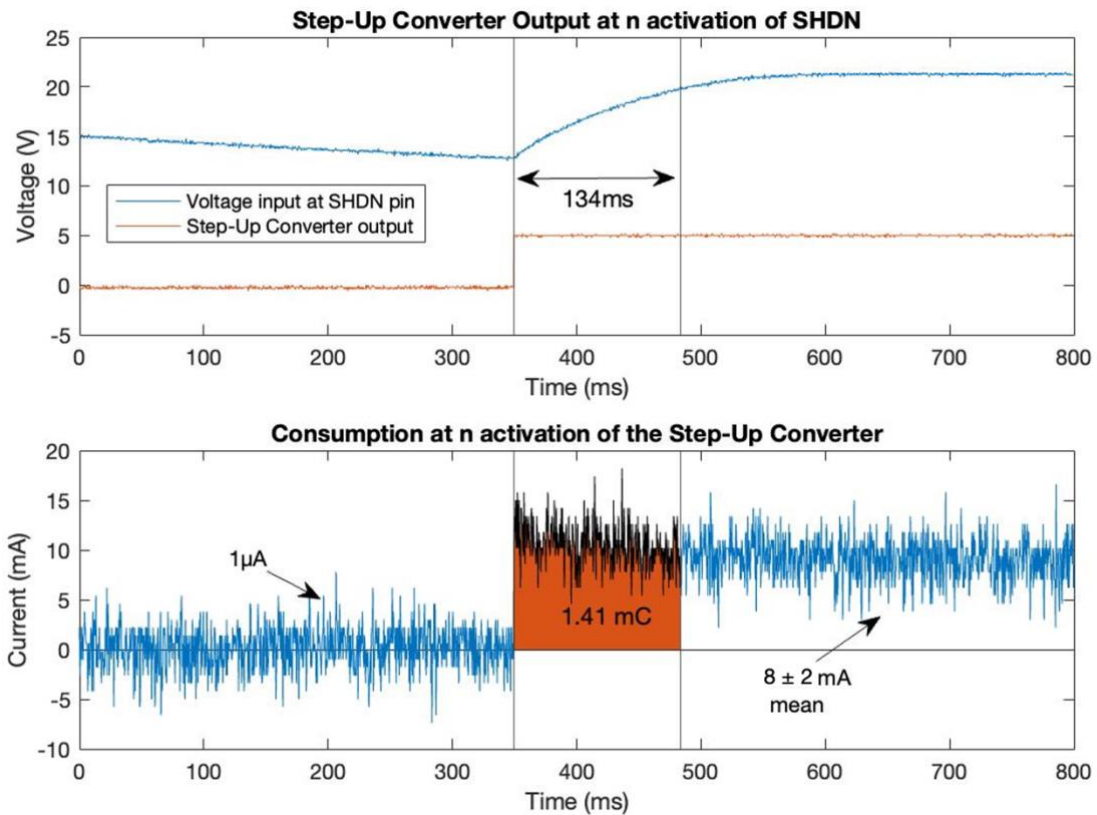


**Figure 28.** Plots of the  $V_{out}$  response and current consumption at the reactivation of the Step-Up Converter starting at 12.2 V.

In this case, rising from 12.2 V instead of from 3 V, the charge consumption is lower and has a value of 1.41 mC, and so is the current after it has reached the 20 V again ( $8 \pm 2$  mA). Due to time constraints the consumption for the rising from 6.2 V could not be measured. The current consumption spared compared to when rising from 3 V is considered negligible and thus 2.15 mC will be assumed.

It is important noting that the rising times will lengthen with worn out batteries and therefore more time is possible to be required to reach 6.2 V, 12.2 V and 20 V. This does not happen with the times of voltage decay since the discharge of the C9 capacitor does not depend on the state of the battery.

Regarding the consumption of the Stimulation Block, the experiments explained above have been carried out while there was generation of stimulation pulses. This was because the activation of the current source that generates the pulses influences the timings of rising and decay of the Step-Up Converter's output and indirectly its consumption. Therefore, the inrush current of the current consumption while stimulating is included in the explained calculations. Moreover, the consumption due to the generation of voltage pulses that control the MOSFETs was also initially thought as a

point of current loss, and the approach of providing the voltage at the gate of the MOSFET2 the minimum time possible that permitted the discharge of the blocking capacitor was conceived (related to (2) *Discharge of blocking capacitor*). However, no consumption due to the generation of those pulses was observed and there was no difference in consumption when applying shorter MOSFET2 control pulses (at least that could be seen in the experiments). Therefore the consumption due to the generation of voltage pulses that control the MOSFET is considered negligible.

The results of the explained evolution and consumption for the Step-Up Converter activation and deactivation are summarized in table 5 of the 5.3. *Results* section.

## **b) Protocol design for the activation of the different blocks aiming to optimize consumption**

The purpose of this VN stimulator is to develop an implantable device suitable for chronic VNS for animal models. The investigation that can be carried out with this VN stimulator can be addressed to treat and study different conditions, which require different VNS parameters. The circuit of this VN stimulator must therefore be able to deliver VNS with different parameters, that will be programmed with the MCU. The activation protocol of the subcircuits has been studied for the two most recurrent VNS guidelines (see Table 1 at 2.1.2.3. *Parameters of Stimulation*).

### **i. FDA guideline for epilepsy**

The parameters to stimulate according with the FDA guideline [20] are:

- Amplitude of stimulation = 1 mA
- Pulse Width = 500  $\mu$ s
- Frequency = 20 Hz
- Period = 50 ms
- Duty Cycle (ON/OFF) = 30 s ON / 5 min OFF

During the 5 min OFF where the Step-Up conversion is not necessary, there will be a total deactivation of this Voltage Booster Block because, as explained in the previous section, it has a very large current consumption and therefore is the component responsible for wearing out the battery. The consumption during this time will be the basal 1  $\mu$ A.

During the 30 s ON, given that the period is of 50 ms, there will be 600 “stimulation cycles” of 50 ms: In one “stimulation cycle” we have a stimulation pulse of 500  $\mu$ s, when MOSFET1 activates the current source and 1 mA is delivered at the electrodes, followed by 49.5 ms in which MOSFET2 deactivates the current source and no stimulation is given. Stimulation pulses are therefore given every 50 ms and they can only be given if the Step-Up Converter has an output of at least 12.2 V.

This section therefore studies the possible patterns of activation and deactivation of the Step-Up Converter, which are referred to as protocols. The activation protocol must be designed to ensure



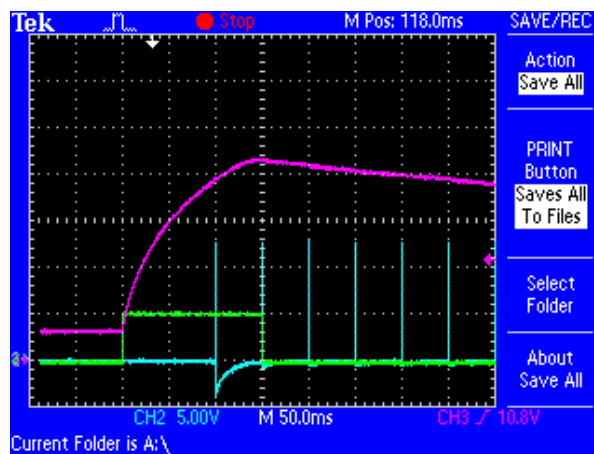
that during these 500  $\mu\text{s}$  stimulation pulses the Step-Up Converter is outputting a minimum of 12.2 V, with the minimum consumption possible.

The simplest option consists in switching on SHDN once and holding the Step-Up Converter active during the whole 30 s ON, having always equal or more than 12.2 V. Then switching it off for the OFF phase. As explained in the previous section, the constant current consumption of the Step-Up Converter after it has stabilized is very high, between 8 and 15 mA, depending on how much time has passed since it has been activated for the first time. During a single whole duty cycle (ON and OFF) this would take up 451.7 mC, which is indeed too much for the use of a small non-rechargeable battery.

Another option that one might consider is activating the Step-Up Converter only when the stimulation pulses are being delivered. This however makes no sense, first because the time that it takes for the Step-Up Converter's output to raise is larger than the period of stimulation and second because the consumption of switching on SHDN after having been switched off is the most expensive, and doing so repeatedly would definitely run down the battery.

Therefore, other strategies based on the slow discharge of C9 must be taken into consideration. These strategies that take advantage of the time that SHDN is off but C9 has still enough charge to output the necessary voltage.

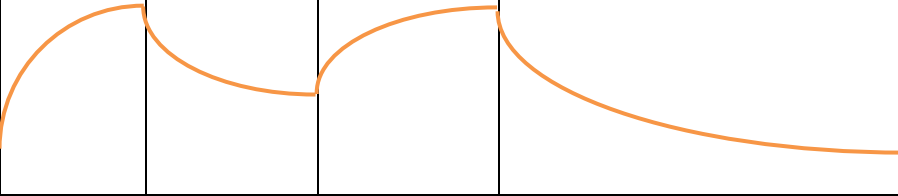
The best strategy to minimize current consumption is detailed in table 4 and is the following: Since stimulation can be delivered as long as  $V_{\text{out}} \geq 12.2 \text{ V}$ , during the first activation of SHDN, it is not necessary to wait until the 20 V are reached, but stimulation can be delivered once the 12.2 V have passed. The first pulse will therefore be delivered during this period of time (figure 29).



**Figure 29.** Screen shot of the oscilloscope.  $V_{\text{out}}$  of the Step-Up Converter in purple (5 V/div). Voltage at SHDN pin in green (5 V/div). Stimulation pulses in blue (5 V/div). Phase A and start of phase B of the stimulation protocol for FDA guideline.

Once  $V_{\text{out}}$  reaches its maximum ( $>20 \text{ V}$ ) SHDN will be switched off and the 1.2 s that take to decay to 12.2 V are used to deliver stimulation. Then, SHDN is switched on again.



Repeat for i in range [1,22]					
PHASE	A First Step-Up Converter Activation	B Step-Up Converter Deactivation	C n – Step-Up Converter Activation	D Last Step-Up Converter Deactivation	
Time interval (ms)	[-100,50)	[50,1250) + 1350·(i-1)	[1250,1400) + 1350·(i-1)	[29.75,30) · 10 <sup>3</sup>	[30,329.9) · 10 <sup>3</sup>
Δ time (ms)	150	1200	150	300.15 · 10 <sup>3</sup>	
SHDN state	ON	OFF	ON	OFF	
Step-Up Converter Output (V) (not at scale)	3 → 20	20 → 12.2	12.2 → 20	20 → 3	
					
Charge Q (μC)	2150	1.2	1410	300.15	
Number of delivered pulses	1	24	3	5	0
Number of times phase must be repeated	1	22		1	

**Table 4.** Consumption phases of the optimal protocol for delivering the treatment according to the FDA stimulation guideline. Where the first pulse is delivered at  $t_0 = 0$ .  
Where  $i \in [1,22]$  and is the number of repetition of the phase (counter).

After the last repetition of the C phase, there will be an additional phase of Step-Up Converter deactivation in which 5 final pulses will be delivered in 250 ms (which belong of course to the 30 s ON). For the computation of the whole consumption, the basal consumption of these 250 ms (01 μA) will be added to the 5 min OFF. However, since the first Step-Up Converter activation starts 100 ms before the first pulse, this basal consumption will not last for 5 min and 0.25 s, but 5 min and 0.15 s instead. This phase of 5 min and 0.15 s (300.15 s) in which consumption is of 1 μA is phase D.

Therefore, during a single duty cycle of 30 s ON and 5 min OFF, the consumption following this protocol is:

$$Q_A + 22 \cdot Q_{B+C} + Q_D = 2.15 + 22 \cdot (1.2 \cdot 10^{-3} + 1.41) + 300.15 \cdot 10^{-3} = 33.50 \text{ mC}$$

To summarize the timings:

During the 30 s ON in which pulses are delivered, the protocol includes the last 50 ms of phase A, 22 consecutive repetitions of complete B and C phases and the first 250 ms of the last D phase. During the 5 min OFF in which no pulses are delivered, the protocol includes the rest of the phase D and the first 100 ms of phase A.

## ii. Rodent model treatment suggested in [21]

The parameters to stimulate according with this guideline are:

- Amplitude of stimulation = 500  $\mu\text{A}$
- Pulse Width = 250  $\mu\text{s}$
- Frequency = 10 Hz
- Period = 100 ms
- Duty Cycle (ON/OFF) = 1 minute ON / 5 min OFF

During the 60 s ON, given that the period is now of 100 ms, there will also be 600 “stimulation cycles” of 100 s: in one “stimulation cycle” there will be a cathodic pulse of 250  $\mu\text{s}$  followed by the anodic wave of 99.75 ms. Stimulation pulses are therefore given every 100 ms and, as explained previously, by voltage compliance they can only be delivered if the Step-Up Converter has a minimum output of 6.2 V. After these 60 s of pulse delivery, there are 5 min OFF of resting state.

With this stimulation parameters, the overall delivered charge of stimulation during the ON phase is less than with the FDA guideline (75 $\mu\text{C}$  compared to 300 $\mu\text{C}$ ). Hence, one might expect that the consumption and battery lifespan should be more satisfactory when stimulating with these parameters. However, it must be stressed that the element that consumes the most is the Step-Up Converter, instead of the Stimulation Block. If the best strategy consisted in activating the Step-Up Converter only when the stimulation pulses are being delivered, the consumption with these parameters would be less, but as has been explained before this protocol is unreasonable. What is relevant is the minimum output voltage for stimulation and time fraction in which the Voltage Booster Block must be outputting this voltage. First of all, this time is in fact unfavourably larger than with the previous parameters (60 s every 5 min instead of 30 s every 5 min). However, the amplitude of the current compared to the FDA guideline’s parameters is lower, demanding a lower minimum output voltage of the Step-Up Converter to stimulate (6.2 V). The decay time from 20 V to 6.2 V is of course wider than from 20 V to 12.2 V, and more advantage can be taken from phase B, which has the lowest basal consumption. However, the consumed charge to go back to 20 V starting at 6.2 V is greater than starting from 12.2 V, and as mentioned in previous sections it is in fact assumed to be the same as when it is starting from 3 V (see 5.2.a) *Study of current consumption and timings of different blocks of the circuit, their activation and deactivation* for details). The best protocol and its outcome are detailed in table 5 and in the explanations that follow.

Again, the activation protocol must be designed to ensure that during these 250  $\mu\text{s}$  stimulation pulses the Step-Up Converter is outputting a minimum of 6.2 V, with the minimum consumption

possible. The best strategy has the same approach as with the FDA parameters, but now for a 60 s ON / 5 min OFF duty cycle and a minimum 6.2 V of Step-Up Converter Output.

Repeat for i in range [1,20]					
PHASE	A First Step-Up Converter Activation	B Step-Up Converter Deactivation	C n – Step-Up Converter Activation	D Last Step-Up Converter Deactivation	
Time interval (ms)	[-50,100)	[100,2900) + 2950·(i-1)	[2900,3050) + 2950·(i-1)	$[59.1,60) \cdot 10^3$	$[60,359.95) \cdot 10^3$
$\Delta$ time (ms)	150	2800	150	$300.85 \cdot 10^3$	
SHDN state	ON	OFF	ON	OFF	
Step-Up Converter Output (not at scale)	3 → 20 V	20 → 6.2 V	6.2 → 20 V	20 → 3 V	
Charge Q (μC)	2150	2.8	2150	300.85	
Number of delivered pulses	1	28	1 if i is odd 2 if i is even	9	0
Number of times phase must be repeated	1	20		1	

**Table 5.** Consumption phases of the optimal protocol for delivering the treatment according to the rodent model treatment suggested in [21]. Where the first pulse is delivered at  $t_0 = 0$ .

Where  $i \in [1,20]$  and is the number of repetition of the phase (counter).

Since stimulation can be delivered as long as  $V_{out} \geq 6.2$  V, during the first activation of SHDN, it is not necessary to wait until the 20 V are reached, but stimulation can start once these 6.2 V have passed.

In analogy with the protocol for the FDA guideline, after the last repetition of the C phase, there will be an additional phase of Step-Up Converter deactivation in which 9 final pulses will be delivered during 900 ms (which belong of course to the 60 s ON). For the computation of the whole consumption, the basal consumption of these 900 ms (1 μA) will be added to the 5 min OFF. However, since the first Step-Up Converter activation starts 50 ms before the first pulse, this basal consumption will not last for 5 min and 0.9 s, but 5 min and 0.85 s instead. This phase of 5 min and 0.85 s (300.85 s) in which consumption is of 1 μA is phase D.

Therefore, during a single duty cycle of 60s ON and 5 min OFF, the consumption following this protocol is:

$$Q_A + 20 \cdot Q_{B+C} + Q_D = 2.15 + 20 \cdot (2.8 \cdot 10^{-3} + 2.15) + 300.85 \cdot 10^{-3} = 45.51 \text{ mC}$$

To summarize the timings:

During the 60 s ON in which pulses are delivered, the protocol includes the last 100 ms of phase A, 20 consecutive repetitions of complete B and C phases and the first 900 ms of the last D phase. During the 5 min OFF in which no pulses are delivered, the protocol includes the rest of the phase D and the first 50 ms of phase A.

### c) Battery's lifespan estimation

With the application of the optimal protocol, the largest lifespan of the battery can be achieved. For the FDA guideline, the consumption of the selected protocol is of 33.50 mC every 330 s. Given that the battery has a capacity of 108 C, with this protocol the battery will last for 12.32 days. For the Rodent Model guideline, the consumption with the selected protocol is of 45.51 mC every 360 s. The battery will last for 9.88 days (almost 10 days).

## 5.3. Results

The final design of the stimulator includes the components of table 2 and the 3D distribution shown in figures 9, 10 and 11. The stimulator has a diameter of 10.4 mm (without counting in the appendix) and a height of 4.05 mm. It has a total volume of 389.35 mm<sup>3</sup> and weights 1.251 g.

The consumption for the different activation phases of Step-Up Converter of the VN stimulator under stimulation conditions (delivering pulses with the parameters of FDA guideline [20] and the rodent model treatment [21]) are summarized in table 6.

Consumption Phases of the Step-Up Converter	Switched Off	First Activation	Switched On	Deactivation		n Activation	Switched On after n activation
<b>SHDN state</b>	= OFF	→ ON	= ON	→ OFF		→ ON	= ON
	3 constant	3 to 20 rising	≥ 20 constant	≥ 12.2 decay	≥ 6.2 decay	12.2 to 20 rising	≥ 20 constant

<b>Step-Up Converter's Output (not at scale)</b>							
<b>Duration (ms)</b>	-	150 (39.2 to 12.2 V) (7 to 6.2 V)	-	1200	2800	150	-
<b>Consumption current (mA)</b>	0.001	Peak at 30.3	14 ± 2	0.001		Peak at 30.2	8 ± 2
<b>Consumption Charge (mC)</b>	-	2.15	-	-	-	1.41	-

**Table 6.** Summary of consumption phases of the Voltage Booster Block.

The protocols have been designed based on the obtained consumptions and consist of maintaining the voltage of the Step-Up Converter's output above the minimum compliance voltage during the ON phases, taking advantage of the discharge time of the C9 capacitor when SHDN is off, when the basal minimum current is being consumed. These protocols are detailed in tables 4 and 5. By following them, the battery lifespan is optimized and lasts up to 12.32 days if the FDA treatment for epilepsy is applied and 9.88 days if the stimulation is being delivered according to the Rodent Model guideline.

## 6. Execution Chronogram (GANTT)

In this section, both a GANTT timing plot of the global project and a GANTT for the specific project of this TFG are reported.

### 6.1. Execution Chronogram of the Global Project

To design the GANTT timing plot, the start and deadline programmed for each stage and their duration must be described (table 7). The global project has a duration of 3 years and is expected to be finished by September 2023.

Stage	Description	Start date	Duration (months)	Final Date
Stage I	Conception of the implantable Vagus Nerve Stimulator, including basic electronic architecture.	September 1 <sup>st</sup> , 2020	10	June 30 <sup>th</sup> , 2021
Stage II	Minimization of volume, weight, and consumption of the stimulator. Protocol design.	September 1 <sup>st</sup> , 2021	5	January 31 <sup>st</sup> , 2022
Stage III	Software programming. MCU and external communication.	February 1 <sup>st</sup> , 2022	5	June 30 <sup>th</sup> , 2023
Stage IV	Electrode development.	September 1 <sup>st</sup> , 2022	5	January 31 <sup>st</sup> , 2023
Stage V	Stimulator encapsulation. Final development of the implant and first pre-clinical studies.	February 1 <sup>st</sup> , 2023	7	August 30 <sup>th</sup> , 2023

**Table 7.** Tasks involved in the realization of the global project of the development of an implantable vagus nerve stimulator.

The visualization of the programming of the global project is shown in the GANTT execution chronogram (figure 30).

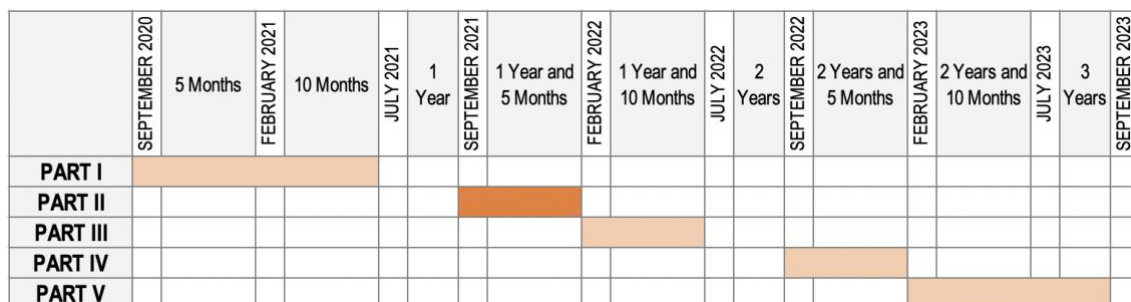


**Figure 30.** GANTT diagram of the global project of the development of an implantable vagus nerve stimulator. In darker orange Stage II constitutes this TFG.

## 6.2. Execution Chronogram of Stage II of the global project

The temporal situation of this TFG (Stage II of the global project) is in darker orange in and comprises the tasks specified in table 8.

Task	Description	Start date	Duration (weeks)	Final Date
A	Project Management	September 1 <sup>st</sup> , 2021	20	January 28 <sup>th</sup> , 2021
B	Conception Engineering	September 6 <sup>th</sup> , 2021	2	September 19 <sup>th</sup> , 2021
C	Revision and reselection of electronic components	September 20 <sup>th</sup> , 2021	2	October 3 <sup>rd</sup> , 2021
D	3D design of the stimulation board	October 4 <sup>th</sup> , 2021	1	October 10 <sup>th</sup> , 2021
E	Study of the electronic behaviour with new components in the evaluation board	October 11 <sup>th</sup> , 2021	3	October 31 <sup>th</sup> , 2021
F	Study of current consumption and timings of different blocks of the circuit, their activation and deactivation.	November 1 <sup>st</sup> , 2021	4	November 28 <sup>th</sup> , 2021
G	Protocol design for the activation of the different blocks aiming to optimize consumption.	November 22 <sup>nd</sup> , 2021	3	December 12 <sup>th</sup> , 2021
H	Battery lifespan estimation.	December 13 <sup>th</sup> , 2021	1	December 19 <sup>th</sup> , 2021
I	Finalization: Handover and presentation.	January 3 <sup>rd</sup> , 2022	3	January 28 <sup>th</sup> , 2022

**Table 8.** Tasks involved in this TFG the Stage II of the global project.

The timings of the tasks that must be carried out during this TFG are shown in its GANTT execution chronogram (figure 31).

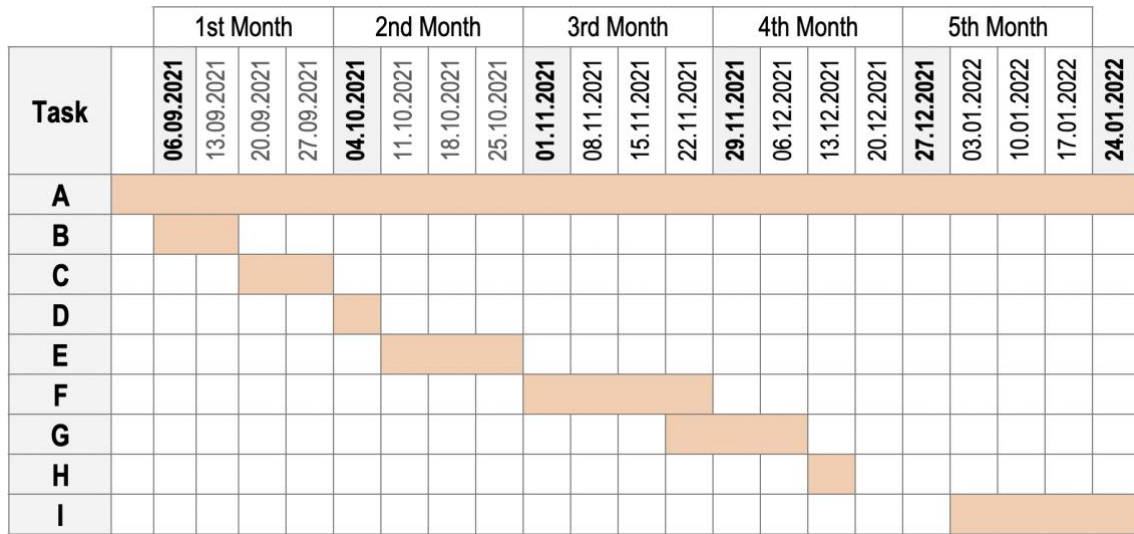


Figure 31. GANTT diagram of Stage II of the global project.



## 7. Technical feasibility: SWOT analysis

The technical feasibility of the global project is described in the SWOT analysis below (table 9).

Internal Analysis	<p style="text-align: center;"><u>Strengths</u></p> <ul style="list-style-type: none"> <li>· High motivation and dynamism of the authors</li> <li>· Clear definition of the project and its global objectives</li> <li>· Guidance and support of top scientists</li> <li>· Powerful laboratories where to develop the implantable VN stimulator</li> </ul>	<p style="text-align: center;"><u>Weaknesses</u></p> <ul style="list-style-type: none"> <li>· High complexity, technically challenging</li> <li>· Lack of experience of the authors on the field</li> <li>· Lack of expertise of the authors on some technical subjects</li> <li>· Limited time</li> <li>· Limited resources</li> </ul>
External Analysis	<p style="text-align: center;"><u>Opportunities</u></p> <ul style="list-style-type: none"> <li>· Release of new products with improved features and/or smaller dimensions that can enhance the stimulator</li> <li>· Good reception of the VN stimulator by research groups</li> </ul>	<p style="text-align: center;"><u>Threats</u></p> <ul style="list-style-type: none"> <li>· Changes in the stipulated guidelines of optimal stimulation that demand changes and remaking some parts of the stimulator</li> <li>· Healthcare regulation changes</li> <li>· Appearance of new VN stimulators in the market</li> <li>· Transcutaneous VN stimulators may take over implantable VN stimulators</li> </ul>

**Table 9.** SWOT analysis of the global project of the development of an implantable vagus nerve stimulator.

In order to take the maximum advantage of the opportunities and to avoid threats as much as possible, the confluence of strengths and opportunities and of weaknesses and threats must be studied.

The internal strengths must be focused to fit with the opportunities. The high dynamism of the authors can be exploited to constantly check market updates on electronical products. These products may possess new characteristics that beat the ones of the products being implemented. This adaptability and disposition to change will then be positive to integrate these new components in substitution of the old ones. The other opportunity, which is the possibility of a positive reception of the VN stimulator in investigation, can be chased with the recommendations of the top scientists

that support the project. Their expertise in the field gives them knowledge about what is being demanded, and the project can be redirected to satisfy it. This will get the project closer to a positive reception of the final VN stimulator by researchers in the field.

Regarding the threats, they cannot be avoided. However, strategies can be thought to control them and actuate as soon as possible so their consequences are the least damaging possible if they appear. The fact that there can be changes in healthcare regulations and in the guidelines of optimal stimulation can be a real problem, given the high complexity of the project and the lack of expertise of the authors. Because of these two weaknesses, the project needs great effort and many hours of devotion, and a remaking can be very challenging. Also, the limitations in time and cost would be problematic. To attenuate effort, time, and economical loss if this circumstance appears, working with the evaluation board instead of with the final stimulation board is a solution. Changes in the evaluation board are easier to make and the final miniaturized stimulation board will be designed and developed only during final steps of the global project. To cope with the appearance of competitors, the guidance of the top investigators will again be vital, as well as a constant revision of the state of the art of the field to keep on pushing the stimulator to have the best characteristics of the market. Finally, the growth of transcutaneous VNS can underrate the purpose of the project. However, as stated in the introduction, many of the VN mechanisms need to be yet investigated. Many of the differences between implantable and non-invasive stimulators are unknown and the VN stimulator of this TFG could be used to draw comparisons between both types of stimulators. Therefore, this threat can be redirected to give greater purpose to the project.

## 8. Economical feasibility

The economical cost of the global project is difficult to estimate, given that what will be done, and the materials used in the following stages are not yet described with precision. However, the economical cost of this TFG can be estimated, and it is mainly based on the products that will be acquired. The implantable VN stimulator was conceived to use only commercially available components, rather than using of much more expensive application-specific integrated circuit (ASIC). The products involved in Stage II of the project and their costs are specified in table 10.

Product	Description	Unit price (€)	# Units	Price (€)
Arduino Uno	Microcontroller	20	1	20
Renata CR1025	Battery	1.8	10	10.80
Abracon ASPI-0315FS-4R7M-T2	Inductor	0.532	10	5.32
Analog Devices LT3467	Boost converter	0.422	10	4.22
Nexperia PSSI2021SAY	Current source	0.315	10	3.15
Analog Devices ADA4505-1	Operational Amplifier	0.13	10	1.30
Texas Instruments DRV5032	Hall Effect sensor	0.0723	10	0.723
ON Semiconductors NSR10F40NXT5G	Schottky diode	0.362	10	3.62
Diodes Incorporated DMN2990UFZ	MOSFET transistors	0.348	10	3.48
Capacitors of the packages 0402 and 0603 packages	Ceramic capacitors	0.0045	11	0.0495
Resistances of the 0201 package	Resistances	0.00509	8	0.0407
<b>TOTAL PRICE</b>				<b>52.70</b>

**Table 10.** Costs of the products and total cost of Stage II of the project.

The packages of the capacitors and resistances are already in the lab and what is taken into consideration is the cost of the number of capacitors and resistors to use alone. The fabrication of the PCB used during this stage was carried out during Stage I of the project and is therefore considered in its budget and not in this one. The authors are not paid since their participation in the project is part of their academic learning. Therefore, the total price is of 52.70€ and is assumed by the Biomedical Electronics Research Group of the Universitat Pompeu Fabra. Stage II of the project is therefore economically viable.

After having developed the project, the prices of the NMOS transistor (BS170 / MMBF170 N) and the electrolytic capacitor (Vishay 517D105M050JA6AE3) which were not expected to be used can be added up to know the exact cost of the project. These are 0.42€ and 0.43€ respectively, summing up a total of 53.55€.

## 9. Regulations and legal aspects

If used in humans, this implantable VN stimulator would be considered an active implantable medical device (AIMD). AIMD is defined as “any active medical device which is intended to be totally or partially introduced, surgically or medically, into the human body or by medical intervention into a natural orifice, and which is intended to remain after the procedure”. It is one of the highest risk categories and hence are subject to rigorous standards and requirements.

The requirements that AIMDs must be defined by the [Regulation \(EU\) 2017/745](#) of the European Parliament and of the Council of 5 April 2017 on medical devices. This regulation has in fact annulled the EU Directive on Active Implantable Medical Devices (90/385/EEC) the past 26th of May of 2021.

The requirements that are generally applicable to AIMDs are specified in the ISO 14708. Also, other standards of safety, quality and efficiency that are not specific for AIMD, but also apply to this VN stimulator are the ones that follow:

- For hardware of medical devices:
  - the ISO 13485:2016 for quality management,
  - the ISO 10993-1:2018 for biological evaluation of medical devices,
  - the ISO 14971:2020 for application of risk management to medical devices and
  - the ISO 15223 for symbols to be used with medical device labels, labelling and information to be supplied.
- For software:
  - the IEC 62304 sets a standard for medical device software.
- Standards are also described for sterilization in the ISO 14937, ISO 11135, ISO 11737-2:2019, and ISO/TS 21387:2020.

## 10. Conclusion and future lines

The dimensions and weight of the proposed 3D stimulator design (389.35 mm<sup>3</sup> and 1.251 g) are satisfactory given that they are competitive with the commercially available stimulators (398.2 mm<sup>3</sup> and 1.4 g by Invilog Research Ltd. and 15 mm of length and 1.2 g by Harald Straus Scientific [30]). The current consumption of the electronic circuit has room for improvement. The block that consumes the most is by large the Step-Up Converter. However, current batteries will be able to feed an implantable stimulator for 12.32 days and 9.88 days of stimulation following the FDA guideline for epilepsy [20] and the rodent model treatment suggested in [21], respectively. New strategies to lower this consumption should be tackled in further studies.

With the application of the best protocol, the battery durations obtained are acceptable for research purposes. However, as afore mentioned, the rising time of the voltage output of the Step-Up Converter can lengthen with worn out batteries and more time will be required to reach the desired tensions. This variability can jeopardize the performance of the stimulator if not enough time to reach these values is given. Therefore, in the following stages of the project a control of this voltage is crucial. A constant check of the Vout of the Step-Up Converter and capacitor C9 with an ADC is proposed. Instead of having previously measured the timings from which the protocols are obtained like it is has been done in this TFG, the best strategy will consist in this control of Vout, which will switch SHDN on when the minimum compliance voltage is recorded and switch it off when the maximum 20 V are reached, regardless of the time it takes.

The future lines of the project start with the implementation of Stage III in which the software based on what has been found in this TFG will be programmed. It is advised for the future stages of the project to implement the suggestion of the constant control of C9 voltage.

To conclude, this TFG sets the necessary grounds for the continuity of the project in next stages.

## 11. References

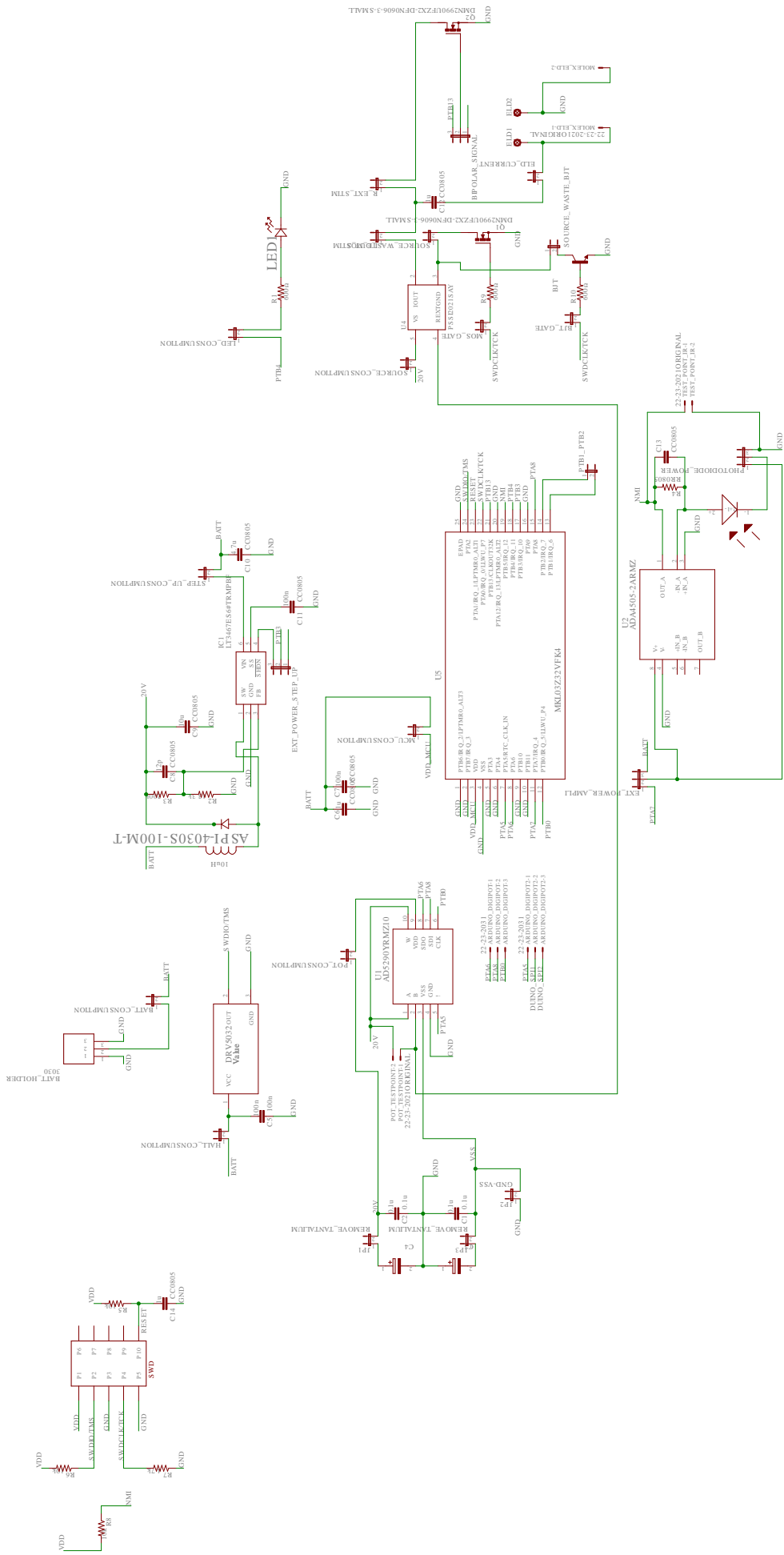
- [1]: Schachter, S. C. (2002). Vagus nerve stimulation therapy summary: Five years after FDA approval. *Neurology*, 59 (Issue 6, Supplement 4), S15-S29. [https://doi.org/10.1212/wnl.59.6\\_suppl\\_4.s15](https://doi.org/10.1212/wnl.59.6_suppl_4.s15)
- [2]: O'Reardon, J. P., Cristancho, P., & Peshek, A. D. (2006). Vagus Nerve Stimulation (VNS) and Treatment of Depression: To the Brainstem and Beyond. *Psychiatry (Edgmont (Pa. : Township))*, 3(5), 54–63.
- [3]: Johnson, R. L., & Wilson, C. G. (2018). A review of vagus nerve stimulation as a therapeutic intervention. *Journal of inflammation research*, 11, 203–213. <https://doi.org/10.2147/JIR.S163248>
- [4]: Bazira, P. J. (2021a). An overview of the nervous system. *Surgery (Oxford)*, 39(8), 451–462. <https://doi.org/10.1016/j.mpsur.2021.06.012>
- [5]: Breit, S., Kupferberg, A., Rogler, G., & Hasler, G. (2018). Vagus Nerve as Modulator of the Brain–Gut Axis in Psychiatric and Inflammatory Disorders. *Frontiers in Psychiatry*, 9. <https://doi.org/10.3389/fpsy.2018.00044>
- [6]: Howland R. H. (2014). Vagus Nerve Stimulation. *Current behavioral neuroscience reports*, 1(2), 64–73.
- [7]: Navin Leanage. (2020). The Vagus Nerve (CN X). TeachMe Anatomy, TeachMe Series.
- [8]: Kenny BJ, Bordoni B. Neuroanatomy, Cranial Nerve 10 (Vagus Nerve). 2021 Nov 14. In: StatPearls [Internet]. Treasure Island (FL): StatPearls Publishing; 2022 Jan–. PMID: 30725856.
- [9]: Eljamel, S. (2011). Problem Based Neurosurgery. p.66
- [10]: Walker HK. Cranial Nerve XI: The Spinal Accessory Nerve. In: Walker HK, Hall WD, Hurst JW, editors. *Clinical Methods: The History, Physical, and Laboratory Examinations*. 3rd edition. Boston: Butterworths; 1990. Chapter 64.
- [11]: Howland R. H. (2014). Vagus Nerve Stimulation. *Current behavioral neuroscience reports*, 1(2), 64–73. <https://doi.org/10.1007/s40473-014-0010-5>
- [12]: Noller, C. M., Levine, Y. A., Urakov, T. M., Aronson, J. P., & Nash, M. S. (2019). Vagus Nerve Stimulation in Rodent Models: An Overview of Technical Considerations. *Frontiers in neuroscience*, 13, 911. <https://doi.org/10.3389/fnins.2019.00911>
- [13]: Ruffoli, R., Giorgi, F. S., Pizzanelli, C., Murri, L., Paparelli, A., & Fornai, F. (2011). The chemical neuroanatomy of vagus nerve stimulation. *Journal of chemical neuroanatomy*, 42(4), 288–296. <https://doi.org/10.1016/j.jchemneu.2010.12.002>
- [14]: Seki, A., Green, H. R., Lee, T. D., Hong, L., Tan, J., Vinters, H. V., Chen, P. S., & Fishbein, M. C. (2014). Sympathetic nerve fibres in human cervical and thoracic vagus nerves. *Heart rhythm*, 11(8), 1411–1417. <https://doi.org/10.1016/j.hrthm.2014.04.032>
- [15]: Elliott, R. E., Rodgers, S. D., Bassani, L., Morsi, A., Geller, E. B., Carlson, C., Devinsky, O., & Doyle, W. K. (2011). Vagus nerve stimulation for children with treatment-resistant epilepsy: a consecutive series of 141 cases. *Journal of neurosurgery. Pediatrics*, 7(5), 491–500. <https://doi.org/10.3171/2011.2.PEDS10505>
- [16]: Krahl S. E. (2012). Vagus nerve stimulation for epilepsy: A review of the peripheral mechanisms. *Surgical neurology international*, 3(Suppl 1), S47–S52. <https://doi.org/10.4103/2152-7806.91610>
- [17]: Krahl SE, Senanayake S, Handforth A. (2012). Stimulation of the subdiaphragmatic vagus nerve to suppress generalized seizures in the rat. *Soc Neurosci Abstracts*. 1999;25:1607.
- [18]: Howland R. H. (2014). Vagus nerve stimulation. *Curr. Behav. Neurosci. Rep.* 1 64–73.

- [19]: Henry T. R. (2002). Therapeutic mechanisms of vagus nerve stimulation. *Neurology* 59(6 Suppl. 4), S3–S14.
- [20]: Groves D. A., Brown V. J. (2005). Vagal nerve stimulation: a review of its applications and potential mechanisms that mediate its clinical effects. *Neurosci. Biobehav. Rev.* 29 493–500. 10.1016/j.neubiorev.2005.01.004
- [21]: Noller, C. M., Levine, Y. A., Urakov, T. M., Aronson, J. P., & Nash, M. S. (2019). Vagus Nerve Stimulation in Rodent Models: An Overview of Technical Considerations. *Frontiers in neuroscience*, 13, 911. <https://doi.org/10.3389/fnins.2019.00911>
- [22]: Janszky J, Hoppe M, Behne F, Tuxhorn I, Pannek HW, Ebner A. (2005). Vagus nerve stimulation: Predictors of seizure freedom. *J Neurol Neurosurg Psychiatry*;76:384–9.
- [23]: Errico, J. P. (2018). The Role of Vagus Nerve Stimulation in the Treatment of Central and Peripheral Pain Disorders and Related Comorbid Somatoform Conditions. *Neuromodulation*, 1551–1564. <https://doi.org/10.1016/B978-0-12-805353-9.00132-7>
- [24]: Krahl, S. E., & Clark, K. B. (2012). Vagus nerve stimulation for epilepsy: A review of central mechanisms. *Surgical neurology international*, 3(Suppl 4), S255–S259. <https://doi.org/10.4103/2152-7806.103015>
- [25]: Zabara J. (1992). Inhibition of experimental seizures in canines by repetitive vagal stimulation. *Epilepsia*, 33(6), 1005–1012. <https://doi.org/10.1111/j.1528-1157.1992.tb01751.x>
- [26]: Agnew, W. F., McCreery, D. B., Yuen, T. G., & Bullara, L. A. (1999). Evolution and resolution of stimulation-induced axonal injury in peripheral nerve. *Muscle & nerve*, 22(10), 1393–1402. [https://doi.org/10.1002/\(sici\)1097-4598\(199910\)22:10<1393::aid-mus9>3.0.co;2-e](https://doi.org/10.1002/(sici)1097-4598(199910)22:10<1393::aid-mus9>3.0.co;2-e)
- [27]: Yao, G., Kang, L., Li, J., Long, Y., Wei, H., Ferreira, C. A., Jeffery, J. J., Lin, Y., Cai, W., & Wang, X. (2018). Effective weight control via an implanted self-powered vagus nerve stimulation device. *Nature communications*, 9(1), 5349. <https://doi.org/10.1038/s41467-018-07764-z>
- [28]: Lee, B., Koripalli, M.K., Jia, Y. et al. (2018). An Implantable Peripheral Nerve Recording and Stimulation System for Experiments on Freely Moving Animal Subjects. *Sci Rep* 8, 6115. <https://doi.org/10.1038/s41598-018-24465-1>
- [29]: El Tahry, R., Raedt, R., Mollet, L., De Herdt, V., Wyckhuys, T., Wyckuys, T., Van Dycke, A., Meurs, A., Dewaele, F., Van Roost, D., Doguet, P., Delbeke, J., Wadman, W., Vonck, K., & Boon, P. (2010). A novel implantable vagus nerve stimulation system (ADNS-300) for combined stimulation and recording of the vagus nerve: pilot trial at Ghent University Hospital. *Epilepsy Research*, 92(2-3), 231-9. <https://doi.org/10.1016/j.eplepsyres.2010.10.007>
- [30]: Bard AJ, Faulkner LR. (1980). *Electrochemical methods*. New York: Wiley; p. 19 and 102 [Chapters 1.3.3, 2, 3.5 and 9.1.3]
- [31]: Cogan S. F. (2008). Neural stimulation and recording electrodes. *Annual review of biomedical engineering*, 10, 275–309. <https://doi.org/10.1146/annurev.bioeng.10.061807.160518>
- [32]: Hoffer, Joaquin & Kallesoe, Klaus. (1999). Nerve cuff electrodes for prosthetic and research applications.
- [33]: Hoffer, Joaquin & Kallesoe, Klaus. (2000). How to Use Nerve Cuffs to Stimulate, Record or Modulate Neural Activity. 10.1201/9781420039054.ch5.
- [34]: Marcos Chic. Universitat Pompeu Fabra. (2021, July). Development of an open-source, wireless and implantable vagus nerve stimulator for preclinical studies in mice.

- [35]: Yaghouby, F., Shafer, B., & Vasudevan, S. (2019). A rodent model for long-term vagus nerve stimulation experiments. *Bioelectronics in Medicine*, 2(2), 73–88. <https://doi.org/10.2217/bem-2019-0016>
- [36]: Stauss H. M. (2017). Differential hemodynamic and respiratory responses to right and left cervical vagal nerve stimulation in rats. *Physiological reports*, 5(7), e13244. <https://doi.org/10.14814/phy2.13244>
- [37]: Fitchett, A., Mastitskaya, S., & Aristovich, K. (2021). Selective Neuromodulation of the Vagus Nerve. *Frontiers in neuroscience*, 15, 685872. <https://doi.org/10.3389/fnins.2021.685872>
- [38]: Plachta, D. T., Gierthmuehlen, M., Cota, O., Espinosa, N., Boeser, F., Herrera, T. C., Stieglitz, T., & Zentner, J. (2014). Blood pressure control with selective vagal nerve stimulation and minimal side effects. *Journal of neural engineering*, 11(3), 036011. <https://doi.org/10.1088/1741-2560/11/3/036011>
- [39]: Pečlin, P., & Rozman, J. (2014). Alternative paradigm of selective vagus nerve stimulation tested on an isolated porcine vagus nerve. *TheScientificWorldJournal*, 2014, 310283. <https://doi.org/10.1155/2014/310283>
- [40]: Ugalde, H. R., Le Rolle, V., Bel, A., Bonnet, J. L., Andreu, D., Mabo, P., Carrault, G., & Hernández, A. I. (2014). On-off closed-loop control of vagus nerve stimulation for the adaptation of heart rate. *Annual International Conference of the IEEE Engineering in Medicine and Biology Society. IEEE Engineering in Medicine and Biology Society. Annual International Conference, 2014*, 6262–6265. <https://doi.org/10.1109/EMBC.2014.6945060>
- [41]: Guiraud, D., Andreu, D., Bonnet, S., Carrault, G., Couderc, P., Hagège, A., Henry, C., Hernandez, A., Karam, N., Rolle, V. Le, Mabo, P., PawełMaciejasz, Malbert, C.-H., Marijon, E., Maubert, S., Picq, C., Rossel, O., & Bonnet, J.-L. (2016). Vagus nerve stimulation: state of the art of stimulation and recording strategies to address autonomic function neuromodulation. *Journal of Neural Engineering*, 13(4), 41002. <https://doi.org/10.1088/1741-2560/13/4/041002>
- [42]: Yap, J. Y. Y., Keatch, C., Lambert, E., Woods, W., Stoddart, P. R., & Kameneva, T. (2020). Critical Review of Transcutaneous Vagus Nerve Stimulation: Challenges for Translation to Clinical Practice. *Frontiers in Neuroscience*, 14. <https://doi.org/10.3389/fnins.2020.00284>  
<https://www.frontiersin.org/articles/10.3389/fnins.2020.00284/full>
- [43]: Epilepsy. (2019, 20 junio). World Health Organization. <https://www.who.int/news-room/fact-sheets/detail/epilepsy>
- [44]: Institute of Health Metrics and Evaluation. Global Health Data Exchange (GHDx). GBD Results Tool (2019). <http://ghdx.healthdata.org/gbd-results-tool?params=gbd-api-2019-permalink/d780dffbe8a381b25e1416884959e88b>
- [45]: Fortune Buisness Insights. (2018). Vagus Nerve Stimulation Market Size, Share & Industry Analysis, By Type, By Application and By End User, and Regional Forecast, 2019–2026 (N.o FBI101184). <https://www.fortunebusinessinsights.com/industry-reports/vagus-nerve-stimulation-vns-market-101184>
- [46]: Verified Market Research. (2021, noviembre). Global Vagus Nerve Stimulation Market Size By Product, By Biomaterial, By Application, By Geographic Scope And Forecast (N.o 25760). <https://www.verifiedmarketresearch.com/product/vagus-nerve-stimulation-market/>







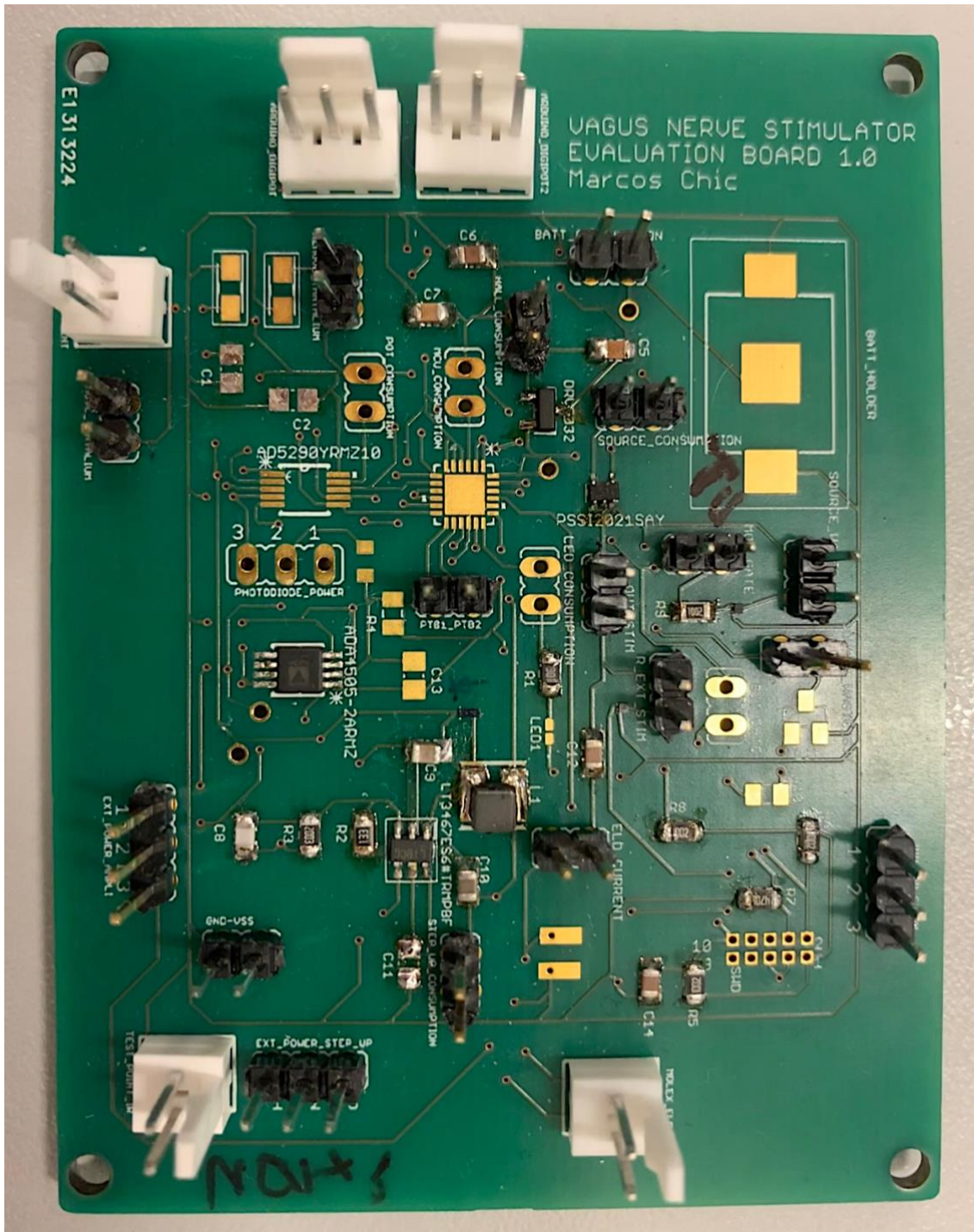


Fig. 3. Evaluation Board of the VN stimulator with the components soldered

```
MOSFET_pulses
void setup() {
    pinMode(8, OUTPUT); // MOSFET1 Gate
    pinMode(12, OUTPUT); // MOSFET2 Gate
}

void loop() {
    // FDA protocol for epilepsy
    digitalWrite(8, HIGH);
    delayMicroseconds(500);
    digitalWrite(8, LOW);
    digitalWrite(12, HIGH);
    delay(49);
    delayMicroseconds(500);
    digitalWrite(12, LOW);
}
```

**Fig. 4.** Basic code for pulse generation according to the FDA guideline. The coding for the control of the Step-Up Converter is not added in this code.

```

clear
%% CONSUMPTION
cons = readtable('21Consumo.csv');
t = cons(:,4); % en s
t = (t - t(1))*1000; % Hacemos que el tiempo empiece en 0 y sean ms
t = round(t,4);
I = cons(:,5)*1000 - 1; % en mA y menos el offset (1mA)
plot(t,I) % Consumo (mA) vs tiempo (ms)
title("Consumption at the activation of SHDN")
xlabel ("Time (ms)")
ylabel ("Current (mA)")
hold on

max(I)

% consumption when SHDN is off (start of the curve)
[ind_1i, ind_1f] = deal(find(t == 0),find(t == 119.8));
consumption_1 = mean(I(ind_1i:ind_1f)); % 0.85mA --> we take the theoretic value

% area under the curve SINCE SHDN HAS BEEN ACTIVATED UNTIL WE REACH 20V
[ind_21i,ind_21f] = deal(find(t == 119.8),find(t == 256));
I21_t2 = I(ind_21i:ind_21f);
t21_t2 = t(ind_21i:ind_21f);
Q_spike = trapz(t21_t2, I21_t2); %mA · ms = uC = 3136uC
area(t21_t2, I21_t2);
hold off

% mean consumption when Output 20V is stable
[ind_22i, ind_22f] = deal(find(t == 119.8),find(t == 499.8));
consumption_22 = mean(I(ind_22i:ind_22f)); % 15.76 mA

%% STEP UP OUTPUT 20V
stepup = readtable('21StepUp_Output.csv');
V_stepup = stepup(:,5); % in V
plot(t,V_stepup,'b-') % Output StepUp (V) vs time (ms)
title("Step Up Converter Output (V)")
xlabel ("Time (ms)")
ylabel ("Voltage (V)")

ind_122Vi = find(V_stepup == 12.2); % index when V = 12.2V
t_122V = t(ind_122Vi(1)); % 159

%% SHDN
shdn = readtable('21SHDN.csv'); % the time of all csv are the same
V_shdn = shdn(:,5); % in V
plot(t,V_shdn) % SHDN activation (V) vs tome (ms)
title("Activation of SHDN")
xlabel ("Time (ms)")
ylabel ("Voltage (V)")

%% SUBPLOTS: ABOVE 20V y SHDN, BEKOW CONSUMPTION
subplot(2,1,1)
plot(t,V_stepup) % Output StepUp (V) vs time (ms)
title("Step-Up Converter Output at the first activation of SHDN")
xlabel ("Time (ms)")
ylabel ("Voltage (V)")
hold on
plot(t,V_shdn)
hold off
xline(119.8)
xline(159)

```

```

xline(256)
legend('Voltage input at SHDN pin', 'Step-Up Converter output')

subplot(2,1,2)
plot(t,I) % Consumption (mA) vs time (ms)
title("Consumption at the first activation of the Step-Up Converter")
xlabel ("Time (ms)")
ylabel ("Current (mA)")
hold on
area(t21_t2, I21_t2);
xline(119.8)
xline(256) % when we have the 20V
hold off

%% BATTERY
bat = readtable('21Renata.csv');
V_bat = bat(:,5); % in V
plot(t,V_bat) % SHDN activation (V) vs time (ms)
title("Battery Voltage")
xlabel ("Time (ms)")
ylabel ("Voltage (V)")

%% Plots sobrepuestos
figure(2)
yyaxis right
plot(t,I) % Consumption (mA) vs time (ms)
xlabel ("Time (ms)")
ylabel ("Current (mA)")
hold on

yyaxis left
plot(t,V_shdn, 'g-') % SHDN activation (V) vs time (ms)
xlabel ("Time (ms)")
ylabel ("Voltage (V)")
hold on

yyaxis left
plot(t,V_stepup, 'b-') % Output StepUp (V) vs time (ms)
xlabel ("Time (ms)")
ylabel ("Voltage (V)")
title ('Consumption measured with current probe at the Step-Up Converter activation')

yyaxis left
plot(t,V_bat, 'y-') % Battery Voltage (V) vs time (ms)
xlabel ("Time (ms)")
ylabel ("Voltage (V)")
hold on

hold off
ax = gca; % black y axis
ax.YAxis(1).Color = 'k';

legend('Voltage input at SHDN pin', 'Step-Up Converter output', 'Battery Voltage',
'Consumption current')

%% Times until 20V
figure(3)
plot(t,V_shdn) % V to SHDN (V) vs time (ms)
hold on
plot(t,V_stepup) % Output StepUp (V) vs time (ms)

```

```

xline(27.16)
xline(28.88)
xline(55)
title("Step Up Converter's Output Response at the activation of SHDN")
xlabel ("Time (ms)")
ylabel ("Current (V)")
legend('Voltage input at SHDN pin','Step-Up Converter output')
hold off

%% If we consider a square consumption at rising
Imax = max(I);
[i_tf, i_to] = deal(find(t == 55),find(t == 28.88)); % indexes of boundary of our
rectangle
I_considered = zeros(length(t),1); % vector of same length than t, one column, full of
0
I_considered(i_to:i_tf,:) = Imax; % in the positions of intensity rising we take Imax
of value
plot(t,I),title("Consumption at the activation of SHDN"), xlabel ("Time (ms)", ylabel
("Current (mA)")
hold on % Consumption (mA) vs time (ms)
plot(t, I_considered)
hold off

```

**Fig. 5.** Example of MATLAB code for measurements and plot generation from data obtained with the oscilloscope. A different code was used for different phases of activation studied.